Journal of Applied Analysis and Computation
Volume 16, Number 4, August 2026, 1756–1783

Website:http://www.jaac-online.com
DOI:10.11948/20250259

EXPLORING THE IMPACT OF MULTIPLICATIVE NOISE ON THE SOLITON DYNAMICS IN THE FRACTIONAL BREAKING SOLITON EQUATION

Parvaiz Ahmad Naik[1,†], Manzoor Ahmad[2,†], Dowlath Fathima[3] and Akbar Zada[2]

Abstract This paper investigates the fractional space-time stochastic $(2+1)$-dimensional breaking soliton equation (FSTSBSE) using the M-truncated fractional derivative. We apply the Generalized Kudryashov-Auxiliary-Jacobian Method (GKAJM) to obtain exact solutions of the FSTSBSE. Several classes of analytical solutions, including trigonometric and hyperbolic forms, are derived. The solutions presented in this study extend and generalize various results previously reported in the literature. Moreover, Maple is employed to generate contour and three-dimensional plots of the obtained fractional-stochastic solutions, providing insight into the influence of multiplicative noise and the M-truncated fractional derivative on the behavior and symmetry of the FSTSBSE solutions. In general, the inclusion of a noise term that breaks solution symmetry tends to enhance stability. Since the combination of fractional spatial effects and multiplicative noise via the proposed approach has not previously been applied to this system, earlier related results are treated as special cases within our more general framework.

Keywords Generalized Kudryashov-Auxaliry-Jacobian method, M-truncated fractional derivative, fractional space-time stochastic dimensional breaking soliton equation, soliton solutions.

MSC(2010) 34K37, 35C08, 35Q51, 35R11.

1. Introduction

The use of stochastic partial differential equations (SPDEs) to model processes in physics, biology, fluid mechanics, oceanography, chemistry, and atmospheric science has increased significantly [8, 19, 23, 46, 63]. In parallel, fractional derivatives have proven effective in representing a wide range of physical phenomena, with applications in physics [2, 5, 45, 60, 68, 80], biology [13, 26, 31, 32, 59, 66, 67, 79], biochemistry and chemistry [54, 78], finance [18, 64, 75] and hydrology [7, 41]. One of the key advantages of fractional derivatives is that they can be viewed as a generalization of classical derivatives; thus, they are capable of describing behaviors that ordinary derivatives cannot [62].

†The corresponding authors.
[1]School of Mathematical Sciences, Chengdu University of Technology, Chengdu 610059, Sichuan, China
[2]Department of Mathematics, University of Peshawar, Peshawar, Khyber Pakhtunkhwa, Pakistan
[3]Basic Sciences Department, College of Science and Theoretical Studies, Saudi Electronic University, Riyadh, Saudi Arabia
Email: naik2026@cdut.edu.cn(P. A. Naik), manzoor930ahmad@uop.edu.pk(M. Ahmad), d.fathima@seu.edu.sa(D. Fathima), zadababo@yahoo.com(A. Zada).

In recent years, numerous analytical and numerical techniques have been developed for solving fractional differential equations. For instance, deterministic fractional partial differential equations (PDEs) have been studied extensively in [9, 10, 17, 28–30, 39, 73, 77], while SPDEs of integer order have been investigated in [27, 49–51, 55, 57]. Additional research on approximate solutions of fractional SPDEs can be found in works, such as Kamrani [34], Taheri et al. [72], Liu and Yan [42], Mohammed [47, 56], Liu [40], Ali et al. [3] and Zou [83]. However, only a limited number of studies, such as [52, 53] have explored exact analytical solutions for fractional SPDEs. This gap highlights the importance of further examining fractional PDE models influenced by random forces.

Motivated by this need, we investigate a stochastic fractional space-time breaking soliton equation of this type, following the structure introduced in [74]. Thus, the fractional space-time stochastic breaking soliton equation FSTSBSE considered in this work is given by:

$$\begin{cases} \mathcal{D}^{\alpha,\beta}_{M,x}\varphi_t - 4\mathcal{D}^{2\alpha,\beta}_{M,x}(\mathcal{D}^{\alpha,\beta}_{M,y}\varphi) - 2\mathcal{D}^{2\alpha,\beta}_{M,x}\varphi\mathcal{D}^{\alpha,\beta}_{M,y}\varphi + \mathcal{D}^{3\alpha,\beta}_{M,x}(\mathcal{D}^{\alpha,\beta}_{M,y}\varphi) \\ =\rho\mathcal{D}^{\alpha,\beta}_{M,x}\varphi\mathcal{B}_t,\ 0 < t, \alpha \in (0,1],\ \beta > 0, \end{cases} \tag{1.1}$$

where $\varphi(x,y,t)$ is a real-valued stochastic function, $\mathcal{D}^{\alpha,\beta}_{M,(\cdot)}$ is the α^{th} order M-truncated fractional derivative, ρ is the noise strength and $\mathcal{B}_t = \frac{d\mathcal{B}(t)}{dt}$ is the time derivative of the standard Bronian motion (Bm), $\mathcal{B}(t)$. The $(2+1)$-dimensional interaction between a long wave propagating along the x-axis and a Riemann wave traveling along the y-axis is described by the breaking soliton equations (BSEs). These equations, in their classical form with BSEs (1.1) with $\alpha = 1$, $\beta = 0$ and $\rho = 0$ are commonly used in the study of shallow-water hydrodynamics, leading fluid flows and plasma physics. However, real physical systems are rarely perfectly deterministic; they are often influenced by fluctuations such as thermal noise, turbulent disturbances, and measurement uncertainties. Incorporating multiplicative stochastic forcing into the breaking soliton equation allows us to capture these realistic perturbations and to study how randomness affects wave stability, symmetry, and propagation. Moreover, extending the model to include fractional spatial derivatives provides an additional degree of freedom for describing memory effects and anomalous diffusion, which cannot be captured by classical derivatives. For these reasons, the FSTSBSE offers a more general and physically meaningful framework for modeling complex nonlinear wave phenomena in multidimensional stochastic environments.

A wide range of analytical techniques has been employed to obtain exact solutions of deterministic BSEs, including the $\tanh - \coth$ method [6], the Hirota bilinear method [24], the improved (G'/G)-expansion, the extended tanh-method [1], the three-wave method [12], Jacobi elliptic function methods [81], the (G'/G)-expansion method, [11], generalized auxiliary equations [82], modified extended direct algebraic method [70] and the Riccati equation method [44]. Despite these developments, exact analytical solutions for the fractional-stochastic breaking soliton equation, including the stochastic perturbation and the shortened M-truncated fractional derivative, remain largely unexplored.

Among the well established analytical techniques, the Exp-function method [4, 15, 21, 43], He's generalized Exp-function method [58], the newly extended auxiliary equation method [35], the modified Kudryashov method [22, 33, 37], Hirotass bilinear method [36], generalized exponential rational function method [61], modified version of extended direct algebraic method [76], the double variable expansion method [65] and the generalized Kudryashov method [16] are particularly notable. Kudryashov [33] initially introduced a wave method involving a rotational function of the form $\frac{a_j}{(1+e^{\eta})^j}$, $j \in \mathbb{N}$. Gaber [16] later enhanced this method by replacing the exponential function e^{ζ} with any function satisfying the Riccati equation, thereby broadening the class of obtainable solutions. In the present work, we further extend Kudryashov's approach by constructing Jacobian elliptic functions through the substitution of e^{η} with an arbitrary function satisfying an auxiliary linear differential equation.

In this article, we consider only the case where the spatial noise is constant. For this reason, it is essential to define the Bm. A Wiener process $\mathcal{B}(t)_{t\geq 0}$ is said to be a Bm, if it satisfies the following conditions [48]:

$$\begin{cases} \mathcal{B}(0) = 0, \\ \mathcal{B}(t) \text{ is a continuous function}, \\ \mathcal{B}(t_2) - \mathcal{B}(t_1) \text{ is independent for}, \ t_2 > t_1, \\ \mathcal{B}(t_2) - \mathcal{B}(t_1) \text{ possess a normal distribution}, \ \mathrm{N}(0, t_2 - t_1). \end{cases}$$

This paper aims to apply the GKAJM to obtain analytical stochastic fractional-space solutions of (1.1). Since the combined effects of multiplicative noise and fractional spatial derivatives have not previously been examined for this system using this method, the results presented here extend and generalize earlier findings. The inclusion of the stochastic term enables us to derive more accurate and physically meaningful solutions. The solutions obtained for (1.1) describe wave phenomena relevant to gravity, nonlinear optics, plasma physics, water waves, and biophysics, thereby offering new insights for modeling complex physical processes. We also analyze the influence of the stochastic term on these solutions. To the best of our knowledge, the analytical soliton solutions presented here for system (1.1) are new and have not been reported elsewhere.

This paper is organized as follows. In the next section, we define the M-truncated fractional derivative and present several of its essential properties. In the section titled The operational procedure of GKAJM for fractional PDEs, we employ a suitable transformation to reduce (1.1) to an ordinary differential equation. The analytical solutions of the resulting system, obtained through the GKAJM, are presented in the section Analytical solution of the nonlinear stochastic fractional space-time breaking soliton system. In the section Discussion and graphs, we provide various graphical illustrations that demonstrate the effect of Bm on the obtained solutions. The Section Conclusion finally concludes this study.

2. Method and materials

2.1. The M-truncated fractional derivative

Using the superior features of the M-truncated fractional derivative versus other fractional derivatives, we may develop traveling wave solutions for fractional PDEs. Notably, the traveling wave solutions for FSTSBSE specified in equation (1.1) cannot be derived using alternate fractional derivative formulations because of their non-compliance with the chain rule [71]. Our main objective of choosing this local derivative is that it encompasses other local derivatives due to containing one additional parameter by virtue of the Mittag-Leffler function. Hence, by iterating this local derivative, we obtain fractional operators with three parameters, providing us with flexibility in observing problems. As a result, we characterize the fractional derivatives used in (1.1) as M-fractional derivatives, [69] defines this derivative operator as:

Definition 2.1. [69] For any function $u : [0, \infty[\to \mathbb{R}$, the truncated M-truncated fractional derivative of α^{th} order, where $\alpha \in (0,1]$ and type β is defined by:

$$\mathcal{D}^{\alpha,\beta}_{M,t}u(t) = \lim_{\tau\to 0}\frac{u(tE_\beta(\tau t^{1-\alpha})) - u(t)}{\tau},$$

where $E_\beta(\cdot)$ is a one parameter Mittag-Leffler function.

Besides, the operator $D^{\alpha,\beta}_{M,t}(\cdot)$ posses the following properties [79]

$$\begin{aligned}
&\mathcal{D}^{\alpha,\beta}_{M,t}u(t) = \frac{t^{1-\alpha}}{\Gamma(1+\beta)}\frac{du(t)}{dt},\\
&\mathcal{D}^{\alpha,\beta}_{M,t}[k_1u(t) \pm k_2v(t) = k_1\mathcal{D}^{\alpha,\beta}_{M,t}u(t) \pm k_2\mathcal{D}^{\alpha,\beta}_{M,t}v(t),\ k_1,\ k_2 \in \mathbb{R},\\
&\mathcal{D}^{\alpha,\beta}_{M,t}\big(u(t)v(t)\big) = u(t)\mathcal{D}^{\alpha,\beta}_{M,t}v(t) + v(t)\mathcal{D}^{\alpha,\beta}_{M,t}u(t),\\
&\mathcal{D}^{\alpha,\beta}_{M,t}\big(\frac{u(t)}{v(t)}\big) = \frac{v(t)\mathcal{D}^{\alpha,\beta}_{M,t}u(t) - u(t)\mathcal{D}^{\alpha,\beta}_{M,t}v(t)}{v^2(t)},\\
&\mathcal{D}^{\alpha,\beta}_{M,t}\big(u\circ v\big)(t) = u'(v(t)\mathcal{D}^{\alpha,\beta}_{M,t}v(t)) = \frac{t^{1-\alpha}u'(v(t))}{\Gamma(1+\beta)}\frac{dv(t)}{dt}.
\end{aligned}$$

3. The operational procedure of GKAJM for fractional PDEs

In this part, we will present the description of the GKAJM.

We study a particular nonlinear partial differential equation related to a function like $\varphi(t, x_1, x_2, x_3 \ldots, x_n)$

$$\Psi(\varphi, D^{\alpha,\beta}_{M,t}\varphi, D^{2\alpha,\beta}_{M,2x}\varphi, D^{2\alpha,\beta}_{M,xt}\varphi, D^{2\alpha,\beta}_{M,2t}\varphi, D^{2\alpha,}_{M,xy}\varphi, \ldots) = 0,\ 0 < \alpha \le 1, \beta > 0, \tag{3.1}$$

where Ψ is a polynomial in φ. We try the wave solution in the form of

$$\varphi(x, y, t) = U(\zeta),\ \zeta = \frac{\Gamma(1+\beta)}{\alpha}(\lambda x^\alpha + \kappa y^\alpha + \mu t^\alpha), \tag{3.2}$$

where λ, κ and μ are constants of the transformation (3.1). Consequently, equation (3.1) is reduced to an ordinary differential equation (ODE):

$$\Phi(U, U', U'', \ldots) = 0. \tag{3.3}$$

The traveling wave solutions can be stated in a certain way, which is the underlying assumption of the GKAJM.

$$U(\zeta) = \sum_{j=-n}^{n}\frac{S_j}{(1+\phi(\zeta))^j}, \tag{3.4}$$

where k is a positive integer to be determined, S_j's are constants. Furthermore, $\phi(\zeta)$ is the solution of auxiliary differential equation given by

$$\phi'(\zeta) = \sqrt{R + Q\phi^2(\zeta) + P\phi^4(\zeta)}. \tag{3.5}$$

The variables R, Q, and P are considered constants in this context. The solutions $\phi(\zeta)$ correspond to Jacobian elliptic functions, which vary based on the specific values assigned to R, Q, and P. Equation (3.5) encompasses a total of 40 distinct solutions [14].

As the parameter m approaches 1, the solutions involving Jacobian elliptic functions transition into hypergeometric functions, demonstrated by the following transformation:

$$\{cn(\zeta), dn(\zeta)\} \to sech(\zeta),\ \{ds(\zeta), cs(\zeta)\} \to cosech(\zeta),\ sn(\zeta) \to \tanh(\zeta),$$
$$\{sc(\zeta), sd(\zeta)\} \to \sinh(\zeta), \{nc(\zeta), nd(\zeta)\} \to \cosh(\zeta),\ ns(\zeta) \to \coth(zeta),\ \{cd(\zeta), dc(\zeta)\} \to 1.$$

The following trigonometric functions are produced when the Jacobian elliptic function solutions are transformed, when the parameter "m" approaches zero:

$$scn(\zeta) \to \tan(\zeta),\ \{cn(\zeta), cd(\zeta)\} \to \cos(\zeta),\ \{sn(\zeta), sd(\zeta)\} \to \sin(\zeta),$$
$$\{nc(\zeta), dc(\zeta)\} \to \sec(\zeta), \{ns(\zeta), ds(\zeta)\} \to \csc(\zeta),\ cs(\zeta) \to \cot(zeta),\ \{dn(\zeta), nd(\zeta)\} \to 1.$$

Table 1. The Jacobian elliptic solutions $\varphi(\zeta)$ of auxiliary equation (3.5).

Cases	R	Q	P	**Solutions**
1	$1-m^2$	$2-m^2$	1	$cs(\zeta)$
2	$\frac{1}{4}$	$\frac{1-2m^2}{2}$	$\frac{1}{4}$	$ns(\zeta) \pm cs(\zeta), \frac{sn(\zeta)}{1 \pm cn(\zeta)}$
3	$\frac{1-m^2}{4}$	$\frac{1+m^2}{2}$	$\frac{1-m^2}{4}$	$nc(\zeta) + sc(\zeta)$
4	1	$2-m^2$	$1-m^2$	$sc(\zeta)$
5	1	$2m^2-1$	$-m(1-m^2)$	$sd(\zeta)$
6	1	$2-4m^2$	1	$\frac{sn(\zeta)dn(\zeta)}{cn(\zeta)}$
7	1	2	m^2	$\frac{sn(\zeta)cn(\zeta)}{dn(\zeta)}$

4. Analytical solution of nonlinear stochastic FSTSBSE interaction system

Here we consider the following wave transformation of Eq. (1.1) given by:

$$\varphi(x,y,t) = U(\zeta)e^{\rho\mathcal{B}(t)-\frac{\rho^2 t}{2}},\ \text{where}\ \zeta = \frac{\Gamma(\beta+1)}{\alpha}\Big(\sigma_1 x^\alpha + \sigma_2 y^\alpha\Big) + t, \tag{4.1}$$

where U is the deterministic function and σ_1, σ_2 are non-zero complex numbers to be determined. Substituting Eq. (4.1) into (1.1) and using

$$\begin{cases} \varphi_t = \dfrac{\partial\varphi(x,y,t)}{\partial t} = (U' + \rho U\mathcal{B}(t) + \dfrac{1}{2}\rho^2 t - \dfrac{1}{2}\rho^2 t)e^{\rho\mathcal{B}(t)-\frac{\rho^2 t}{2}}, \\ \mathcal{D}^{\alpha,\beta}_{M,x}\varphi_t = (\sigma_1 U'' + \rho\sigma_1 U'\mathcal{B}_t)e^{\rho\mathcal{B}(t)-\frac{\rho^2 t}{2}}, \\ \mathcal{D}^{\alpha,\beta}_{M,y}\varphi(x,y,t) = \sigma_2^2 U' e^{\rho\mathcal{B}(t)-\frac{\rho^2 t}{2}}, \\ \mathcal{D}^{\alpha,\beta}_{M,x}\mathcal{D}^{\alpha,\beta}_{M,y}\varphi(x,y,t) = \sigma_1\sigma_2^2 U'' e^{\rho\mathcal{B}(t)-\frac{\rho^2 t}{2}}, \\ \mathcal{D}^{2\alpha,\beta}_{M,x}\varphi(x,y,t) = \sigma_1^2 U'' e^{\rho\mathcal{B}(t)-\frac{\rho^2 t}{2}}, \\ \mathcal{D}^{3\alpha,\beta}_{M,x}\mathcal{D}^{\alpha,\beta}_{M,y}\varphi(x,y,t) = \sigma_1^3\sigma_2 U'''' e^{\rho\mathcal{B}(t)-\frac{\rho^2 t}{2}}, \end{cases} \tag{4.2}$$

to get

$$U'' - 6\sigma_1\sigma_2 U'U'' e^{\rho\mathcal{B}(t)-\frac{\rho^2 t}{2}} + \sigma_1^2\sigma_2 U'''' = 0,\ \text{where,}\ U' = \frac{dU}{d\zeta}. \tag{4.3}$$

Taking expectation E on both sides of (4.3) with the property $\mathrm{E}(e^{\rho\mathcal{B}(t)}) = e^{\frac{\rho^2 t}{2}}$, we obtain

$$U'' - 6\sigma_1\sigma_2 U'U'' + \sigma_1^2\sigma_2 U'''' = 0. \tag{4.4}$$

Integrating this equation (4.4) once w.t.r to ζ and setting the integration constant to zero yields the following solution:

$$U' - 3\sigma_1\sigma_2[U']^2 + \sigma_1^2\sigma_2 U''' = 0. \tag{4.5}$$

Replacing φ' by V in (4.5), we have

$$V - 3\sigma_1\sigma_2 V^2 + \sigma_1^2\sigma_2 V'' = 0. \tag{4.6}$$

We investigate the balance between the highest derivatives V'' and V^2, for a homogeneous integer n as shown in Eq. (4.6), we get $n = 2$. Let the variable V have a series form solution (3.2), with $n = 2$, we get a system of algebraic equations. The application of Maple software yields the solution to this system. Then, afterward, we have two separate sets of answers.

Case 1.

$$\begin{aligned}
&S_{-2} = \sqrt[4]{-\frac{1}{\sigma_2^2(-Q^2+3RP)}}P,\ S_{-1} = -2S_{-2},\\
&S_{-1} = \frac{P\Big(1 + 3\sqrt{\frac{-1}{\sigma_2^2(-Q^2+3RP)}}\sigma_2 P + \sqrt{\frac{-1}{\sigma_2^2(-Q^2+3RP)}}\sigma_2 Q\Big)}{3S_2\sigma_2},\\
&S_1 = S_2 = 0,\ \sigma_2 = \sigma_2,\ \sigma_1 = \frac{S_{-2}}{2P}.
\end{aligned}$$

Case 2.

$$\begin{aligned}
&S_{-2} = \iota\sqrt[4]{-\frac{1}{\sigma_2^2(-Q^2+3RP)}}P,\ S_{-1} = -2S_{-2},\\
&S_{-1} = -\frac{P\Big(-1 + 3\sqrt{\frac{-1}{\sigma_2^2(-Q^2+3RP)}}\sigma_2 P + \sqrt{\frac{-1}{\sigma_2^2(-Q^2+3RP)}}\sigma_2 Q\Big)}{3S_2\sigma_2},\\
&S_1 = S_2 = 0,\ \sigma_2 = \sigma_2,\ \sigma_1 = \frac{S_{-2}}{2P}.
\end{aligned}$$

Assuming the **Case 1**, we get the following families of solutions with the help of Table 1.

Family 1.1. For $R = 1 - m^2$, $\quad Q = 2 - m^2$, $\quad P = 1$.

Case 1. When $m \to 1$,

$$\begin{aligned}
&\varphi_{1,1}(x,y,t)\\
&= e^{\rho\mathcal{B}(t)-\frac{\rho^2}{2}t}\Bigg(\sqrt[4]{-\frac{1}{{\sigma_2}^2(-Q^2+3RP)}}\zeta - 4\sqrt[4]{-\frac{1}{{\sigma_2}^2(-Q^2+3RP)}}\operatorname{arctanh}(\mathrm{e}^{\zeta})
\end{aligned}$$

$$- \sqrt[4]{-\frac{1}{{\sigma_2}^2(-Q^2+3RP)}}\coth(\zeta) - \sqrt[4]{-\frac{1}{{\sigma_2}^2(-Q^2+3RP)}}P\zeta$$
$$- 2\sqrt[4]{-\frac{1}{{\sigma_2}^2(-Q^2+3RP)}}P\ln(\tanh(\frac{1}{2}\zeta)) + \frac{1}{3\sigma_2}\zeta\frac{1}{\sqrt[4]{-\frac{1}{{\sigma_2}^2(-Q^2+3RP)}}}$$
$$+ \frac{1}{3}\sqrt[4]{-\frac{1}{{\sigma_2}^2(-Q^2+3RP)}}\zeta Q\Bigg). \tag{4.7}$$

Case 2. When $m \to 0$,

$$\begin{aligned}
&\varphi_{1,2}(x,y,t)\\
&= e^{\rho\mathcal{B}(t)-\frac{\rho^2}{2}t}\Big(- \sqrt[4]{-\frac{1}{{\sigma_2}^2(-Q^2+3RP)}}\cot(\zeta) - \sqrt[4]{-\frac{1}{{\sigma_2}^2(-Q^2+3RP)}}\ln(1+(\cot(\zeta))^2)\\
&- \sqrt[4]{-\frac{1}{{\sigma_2}^2(-Q^2+3RP)}}P\zeta - 2\sqrt[4]{-\frac{1}{{\sigma_2}^2(-Q^2+3RP)}}P\ln(\sin(\zeta)) + \frac{1}{3\sigma_2}\zeta\frac{1}{\sqrt[4]{-\frac{1}{{\sigma_2}^2(-Q^2+3RP)}}}\\
&+ \frac{1}{3}\sqrt[4]{-\frac{1}{{\sigma_2}^2(-Q^2+3RP)}}\zeta Q\Big).
\end{aligned} \tag{4.8}$$

Family 1.2. For $R = \frac{1}{4}, \quad Q = \frac{1-2m^2}{2}, \quad P = \frac{1}{4}$.

Case 2. When $m \to 1$,

$$\begin{aligned}
&\varphi_{1,3}(x,y,t)\\
&= e^{\rho\mathcal{B}(t)-\frac{\rho^2}{2}t}\Big(2\sqrt[4]{-\frac{1}{{\sigma_2}^2(-Q^2+3RP)}}\zeta + 2\sqrt[4]{-\frac{1}{{\sigma_2}^2(-Q^2+3RP)}}\ln(\sinh(\zeta))\\
&- 4\sqrt[4]{-\frac{1}{{\sigma_2}^2(-Q^2+3RP)}}\operatorname{arctanh}(e^{\zeta}) - \sqrt[4]{-\frac{1}{{\sigma_2}^2(-Q^2+3RP)}}\coth(\zeta)\\
&- 2\sqrt[4]{-\frac{1}{{\sigma_2}^2(-Q^2+3RP)}}\coth(\zeta)\operatorname{csch}(\zeta)\\
&+ 2\sqrt[4]{-\frac{1}{{\sigma_2}^2(-Q^2+3RP)}}\sinh(\zeta) - \sqrt[4]{-\frac{1}{{\sigma_2}^2(-Q^2+3RP)}}\coth(\zeta)\\
&- \sqrt[4]{-\frac{1}{{\sigma_2}^2(-Q^2+3RP)}}P\zeta - 2\sqrt[4]{-\frac{1}{{\sigma_2}^2(-Q^2+3RP)}}P\ln(\sinh(\zeta))\\
&- 2\sqrt[4]{-\frac{1}{{\sigma_2}^2(-Q^2+3RP)}}P\ln(\tanh(\frac{1}{2}\zeta))\\
&+ \frac{1}{3\sigma_2}\zeta\frac{1}{\sqrt[4]{-\frac{1}{{\sigma_2}^2(-Q^2+3RP)}}} + \frac{1}{3}\sqrt[4]{-\frac{1}{{\sigma_2}^2(-Q^2+3RP)}}\zeta Q\Big),
\end{aligned} \tag{4.9}$$

$$
\begin{aligned}
&\varphi_{1,4}(x,y,t)\\
=&e^{\rho\mathcal{B}(t)-\frac{\rho^2}{2}t}\Big(2\sqrt[4]{-\frac{1}{{\sigma_2}^2(-Q^2+3RP)}}\zeta+2\sqrt[4]{-\frac{1}{{\sigma_2}^2(-Q^2+3RP)}}\ln(\sinh(\zeta))\\
&+4\sqrt[4]{-\frac{1}{{\sigma_2}^2(-Q^2+3RP)}}\operatorname{arctanh}(\mathrm{e}^{\zeta})\\
&-\sqrt[4]{-\frac{1}{{\sigma_2}^2(-Q^2+3RP)}}\coth(\zeta)+2\sqrt[4]{-\frac{1}{{\sigma_2}^2(-Q^2+3RP)}}\coth(\zeta)\operatorname{csch}(\zeta)\\
&-2\sqrt[4]{-\frac{1}{{\sigma_2}^2(-Q^2+3RP)}}\sinh(\zeta)-\sqrt[4]{-\frac{1}{{\sigma_2}^2(-Q^2+3RP)}}\coth(\zeta)-\sqrt[4]{-\frac{1}{{\sigma_2}^2(-Q^2+3RP)}}P\zeta\\
&-2\sqrt[4]{-\frac{1}{{\sigma_2}^2(-Q^2+3RP)}}P\ln(\sinh(\zeta))+2\sqrt[4]{-\frac{1}{{\sigma_2}^2(-Q^2+3RP)}}P\ln(\tanh(\frac{1}{2}\zeta))\\
&+\frac{1}{3}\zeta\frac{1}{\sqrt[4]{-\frac{1}{{\sigma_2}^2(-Q^2+3RP)}}}{\sigma_2}^{-1}+\frac{1}{3}\sqrt[4]{-\frac{1}{{\sigma_2}^2(-Q^2+3RP)}}\zeta Q\Big),
\end{aligned}
\tag{4.10}
$$

$$
\begin{aligned}
&\varphi_{1,5}(x,y,t)\\
=&e^{\rho\mathcal{B}(t)-\frac{\rho^2}{2}t}\Big(-2\sqrt[4]{-\frac{1}{{\sigma_2}^2(-Q^2+3RP)}}\tanh(\frac{1}{2}\zeta)-4\sqrt[4]{-\frac{1}{{\sigma_2}^2(-Q^2+3RP)}}\ln(\tanh(\frac{1}{2}\zeta)-1)\\
&-\sqrt[4]{-\frac{1}{{\sigma_2}^2(-Q^2+3RP)}}P\zeta+2\sqrt[4]{-\frac{1}{{\sigma_2}^2(-Q^2+3RP)}}P\ln(\operatorname{sech}(\zeta))\\
&-2\sqrt[4]{-\frac{1}{{\sigma_2}^2(-Q^2+3RP)}}P\ln(1+\operatorname{sech}(\zeta))+\frac{1}{3\sigma_2}\zeta\frac{1}{\sqrt[4]{-\frac{1}{{\sigma_2}^2(-Q^2+3RP)}}}\\
&+\frac{1}{3}\sqrt[4]{-\frac{1}{{\sigma_2}^2(-Q^2+3RP)}}\zeta Q\Big),
\end{aligned}
\tag{4.11}
$$

$$
\begin{aligned}
&\varphi_{1,6}(x,y,t)\\
=&e^{\rho\mathcal{B}(t)-\frac{\rho^2}{2}t}\Big(4\sqrt[4]{-\frac{1}{{\sigma_2}^2(-Q^2+3RP)}}\ln(\tanh(\frac{1}{2}\zeta))-4\sqrt[4]{-\frac{1}{{\sigma_2}^2(-Q^2+3RP)}}\ln(\tanh(\frac{1}{2}\zeta)-1)\\
&-2\sqrt[4]{-\frac{1}{{\sigma_2}^2(-Q^2+3RP)}}\coth(\frac{1}{2}\zeta)-\sqrt[4]{-\frac{1}{{\sigma_2}^2(-Q^2+3RP)}}P\zeta\\
&+2\sqrt[4]{-\frac{1}{{\sigma_2}^2(-Q^2+3RP)}}P\ln(\operatorname{sech}(\zeta))-2\sqrt[4]{-\frac{1}{{\sigma_2}^2(-Q^2+3RP)}}P\ln(-1+\operatorname{sech}(\zeta))\\
&+\frac{1}{3\sigma_2}\zeta\frac{1}{\sqrt[4]{-\frac{1}{{\sigma_2}^2(-Q^2+3RP)}}}+\frac{1}{3}\sqrt[4]{-\frac{1}{{\sigma_2}^2(-Q^2+3RP)}}\zeta Q\Big).
\end{aligned}
\tag{4.12}
$$

Case 2. When $m \to 0$

$$\begin{aligned}
&\varphi_{1,7}(x,y,t)\\
=&e^{\rho\mathcal{B}(t)-\frac{\rho^2}{2}t}\Big(2\sqrt[4]{-\frac{1}{{\sigma_2}^2(-Q^2+3RP)}}\ln(\sec(\zeta)+\tan(\zeta))+2\sqrt[4]{-\frac{1}{{\sigma_2}^2(-Q^2+3RP)}}\ln(\sin(\zeta))\\
&+\sqrt[4]{-\frac{1}{{\sigma_2}^2(-Q^2+3RP)}}\tan(\zeta)+2\sqrt[4]{-\frac{1}{{\sigma_2}^2(-Q^2+3RP)}}\ln(\csc(\zeta)-\cot(\zeta))\\
&-\sqrt[4]{-\frac{1}{{\sigma_2}^2(-Q^2+3RP)}}\cot(\zeta)-\sqrt[4]{-\frac{1}{{\sigma_2}^2(-Q^2+3RP)}}P\zeta-2\sqrt[4]{-\frac{1}{{\sigma_2}^2(-Q^2+3RP)}}P\\
&\times\ln(\sec(\zeta)+\tan(\zeta))-2\sqrt[4]{-\frac{1}{{\sigma_2}^2(-Q^2+3RP)}}P\ln(\sin(\zeta))+\frac{1}{3\sigma_2}\zeta\frac{1}{\sqrt[4]{-\frac{1}{{\sigma_2}^2(-Q^2+3RP)}}}\\
&+\frac{1}{3}\sqrt[4]{-\frac{1}{{\sigma_2}^2(-Q^2+3RP)}}\zeta Q\Big),
\end{aligned}\tag{4.13}$$

$$\begin{aligned}
&\varphi_{1,8}(x,y,t)\\
=&e^{\rho\mathcal{B}(t)-\frac{\rho^2}{2}t}\Big(2\sqrt[4]{-\frac{1}{{\sigma_2}^2(-Q^2+3RP)}}\ln(\sec(\zeta)+\tan(\zeta))-2\sqrt[4]{-\frac{1}{{\sigma_2}^2(-Q^2+3RP)}}\ln(\sin(\zeta))\\
&+\sqrt[4]{-\frac{1}{{\sigma_2}^2(-Q^2+3RP)}}\tan(\zeta)-2\sqrt[4]{-\frac{1}{{\sigma_2}^2(-Q^2+3RP)}}\ln(\csc(\zeta)-\cot(\zeta))\\
&-\sqrt[4]{-\frac{1}{{\sigma_2}^2(-Q^2+3RP)}}\cot(\zeta)-\sqrt[4]{-\frac{1}{{\sigma_2}^2(-Q^2+3RP)}}P\zeta-2\sqrt[4]{-\frac{1}{{\sigma_2}^2(-Q^2+3RP)}}P\\
&\times\ln(\sec(\zeta)+\tan(\zeta))+2\sqrt[4]{-\frac{1}{{\sigma_2}^2(-Q^2+3RP)}}P\ln(\sin(\zeta))+\frac{1}{3\sigma_2}\zeta\frac{1}{\sqrt[4]{-\frac{1}{{\sigma_2}^2(-Q^2+3RP)}}}\\
&+\frac{1}{3}\sqrt[4]{-\frac{1}{{\sigma_2}^2(-Q^2+3RP)}}\zeta Q\Big),
\end{aligned}\tag{4.14}$$

$$\begin{aligned}
&\varphi_{1,9}(x,y,t)\\
=&e^{\rho\mathcal{B}(t)-\frac{\rho^2}{2}t}\Big(2\sqrt[4]{-\frac{1}{{\sigma_2}^2(-Q^2+3RP)}}\tan(\frac{1}{2}\zeta)+2\sqrt[4]{-\frac{1}{{\sigma_2}^2(-Q^2+3RP)}}\ln(\sec^2(\frac{\zeta}{2}))\\
&-\sqrt[4]{-\frac{1}{{\sigma_2}^2(-Q^2+3RP)}}P\zeta+2\sqrt[4]{-\frac{1}{{\sigma_2}^2(-Q^2+3RP)}}P\ln(1+\cos(\zeta))\\
&+\frac{1}{3\sigma_2}\zeta\frac{1}{\sqrt[4]{-\frac{1}{{\sigma_2}^2(-Q^2+3RP)}}}+\frac{1}{3}\sqrt[4]{-\frac{1}{{\sigma_2}^2(-Q^2+3RP)}}\zeta Q\Big),
\end{aligned}\tag{4.15}$$

$$\begin{aligned}&\varphi_{1,10}(x,y,t)\\=&e^{\rho\mathcal{B}(t)-\frac{\rho^2}{2}t}\Big(-2\sqrt[4]{-\frac{1}{{\sigma_2}^2(-Q^2+3RP)}}\ln((\tan(\frac{1}{2}\zeta))^2+1)-2\sqrt[4]{-\frac{1}{{\sigma_2}^2(-Q^2+3RP)}}\cot(\frac{1}{2}\zeta)\\&+4\sqrt[4]{-\frac{1}{{\sigma_2}^2(-Q^2+3RP)}}\ln(\tan(\frac{1}{2}\zeta))-\sqrt[4]{-\frac{1}{{\sigma_2}^2(-Q^2+3RP)}}P\zeta\\&-2\sqrt[4]{-\frac{1}{{\sigma_2}^2(-Q^2+3RP)}}P\ln(1-\cos(\zeta))+\frac{1}{3\sigma_2}\zeta\frac{1}{\sqrt[4]{-\frac{1}{{\sigma_2}^2(-Q^2+3RP)}}}\\&+\frac{1}{3}\sqrt[4]{-\frac{1}{{\sigma_2}^2(-Q^2+3RP)}}\zeta Q\Big).\end{aligned}\tag{4.16}$$

Family 1.3. For $R=\frac{1-m^2}{4}, \quad Q=\frac{1+m^2}{2}, \quad P=\frac{1-m^2}{4}$.

Case 1. When $m\to 1$,

$$\begin{aligned}&\varphi_{1,11}(x,y,t)\\=&e^{\rho\mathcal{B}(t)-\frac{\rho^2}{2}t}\Big(\sqrt[4]{-\frac{1}{{\sigma_2}^2(-Q^2+3RP)}}(\zeta+2\sinh(\zeta)+2\cosh(\zeta)+\cosh(\zeta)\sinh(\zeta)+\cosh^2(\zeta))\\&-2\sqrt[4]{-\frac{1}{{\sigma_2}^2(-Q^2+3RP)}}P(\zeta+\sinh(\zeta)+\cosh(\zeta))\\&+\frac{1}{3\sigma_2}(1+3\sqrt{-\frac{1}{{\sigma_2}^2(-Q^2+3RP)}}\sigma_2P+\sqrt{-\frac{1}{{\sigma_2}^2(-Q^2+3RP)}}\sigma_2Q)\zeta\frac{1}{\sqrt[4]{-\frac{1}{{\sigma_2}^2(-Q^2+3RP)}}}\Big).\end{aligned}\tag{4.17}$$

Case 2. When $m\to 0$,

$$\begin{aligned}&\varphi_{1,12}(x,y,t)\\=&e^{\rho\mathcal{B}(t)-\frac{\rho^2}{2}t}\Big(\sqrt[4]{-\frac{1}{{\sigma_2}^2(-Q^2+3RP)}}\tan(\zeta)+2\sqrt[4]{-\frac{1}{{\sigma_2}^2(-Q^2+3RP)}}\ln(\sec(\zeta)+\tan(\zeta))\\&+2\sqrt[4]{-\frac{1}{{\sigma_2}^2(-Q^2+3RP)}}\sec(\zeta)-2\sqrt[4]{-\frac{1}{{\sigma_2}^2(-Q^2+3RP)}}\ln(\cos(\zeta))+\sqrt[4]{-\frac{1}{{\sigma_2}^2(-Q^2+3RP)}}\\&\times\tan(\zeta)-\sqrt[4]{-\frac{1}{{\sigma_2}^2(-Q^2+3RP)}}P\zeta-2\sqrt[4]{-\frac{1}{{\sigma_2}^2(-Q^2+3RP)}}P\ln(\sec(\zeta)+\tan(\zeta))\\&+2\sqrt[4]{-\frac{1}{{\sigma_2}^2(-Q^2+3RP)}}P\ln(\cos(\zeta))+\frac{1}{3\sigma_2}\zeta\frac{1}{\sqrt[4]{-\frac{1}{{\sigma_2}^2(-Q^2+3RP)}}}\\&+\frac{1}{3}\sqrt[4]{-\frac{1}{{\sigma_2}^2(-Q^2+3RP)}}\zeta Q\Big).\end{aligned}\tag{4.18}$$

Family 1.4. For $R = 1, \quad Q = 2 - m^2, \quad P = 1 - m^2$.

Case 1. When $m \to 1$,

$$\begin{aligned}
&\varphi_{1,13}(x,y,t)\\
=&e^{\rho\mathcal{B}(t)-\frac{\rho^2}{2}t}\Big(\sqrt[4]{-\frac{1}{{\sigma_2}^2(-Q^2+3RP)}}(\frac{1}{2}\zeta+2\cosh(\zeta)+\frac{1}{2}\cosh(\zeta)\sinh(\zeta))\\
&-2\sqrt[4]{-\frac{1}{{\sigma_2}^2(-Q^2+3RP)}}P(\zeta+\cosh(\zeta))\\
&+\frac{1}{3\sigma_2}(1+3\sqrt{-\frac{1}{{\sigma_2}^2(-Q^2+3RP)}}\sigma_2 P+\sqrt{-\frac{1}{{\sigma_2}^2(-Q^2+3RP)}}\sigma_2 Q)\zeta\frac{1}{\sqrt[4]{-\frac{1}{{\sigma_2}^2(-Q^2+3RP)}}}\Big).
\end{aligned} \tag{4.19}$$

Case 2. When $m \to 0$,

$$\begin{aligned}
&\varphi_{1,14}(x,y,t)\\
=&e^{\rho\mathcal{B}(t)-\frac{\rho^2}{2}t}\Big(\sqrt[4]{-\frac{1}{{\sigma_2}^2(-Q^2+3RP)}}\tan(\zeta)+\sqrt[4]{-\frac{1}{{\sigma_2}^2(-Q^2+3RP)}}\ln(sec^2(\zeta))\\
&-\sqrt[4]{-\frac{1}{{\sigma_2}^2(-Q^2+3RP)}}P\zeta+2\sqrt[4]{-\frac{1}{{\sigma_2}^2(-Q^2+3RP)}}P\ln(\cos(\zeta))\\
&+\frac{1}{3\sigma_2}\zeta\frac{1}{\sqrt[4]{-\frac{1}{{\sigma_2}^2(-Q^2+3RP)}}}+\frac{1}{3}\sqrt[4]{-\frac{1}{{\sigma_2}^2(-Q^2+3RP)}}\zeta\, Q\Big).
\end{aligned} \tag{4.20}$$

Family 1.5. For $R = 1, \quad Q = 2m^2 - 1, \quad P = -m(1 - m^2)$.

Case 1. When $m \to 1$,

$$\begin{aligned}
&\varphi_{1,15}(x,y,t)\\
=&e^{\rho\mathcal{B}(t)-\frac{\rho^2}{2}t}\Big(\sqrt[4]{-\frac{1}{{\sigma_2}^2(-Q^2+3RP)}}(\frac{1}{2}\zeta+2\ \cosh(\zeta)+\frac{1}{2}\cosh(\zeta)\sinh(\zeta))\\
&-2\sqrt[4]{-\frac{1}{{\sigma_2}^2(-Q^2+3RP)}}P(\zeta+\cosh(\zeta))\\
&+\frac{1}{3\sigma_2}(1+3\sqrt{-\frac{1}{{\sigma_2}^2(-Q^2+3RP)}}\sigma_2 P+\sqrt{-\frac{1}{{\sigma_2}^2(-Q^2+3RP)}}\sigma_2 Q)\zeta\frac{1}{\sqrt[4]{-\frac{1}{{\sigma_2}^2(-Q^2+3RP)}}}\Big).
\end{aligned} \tag{4.21}$$

Case 2. When $m \to 0$,

$$\begin{aligned}
&\varphi_{1,16}(x,y,t)\\
=&e^{\rho\mathcal{B}(t)-\frac{\rho^2}{2}t}\Big(\sqrt[4]{-\frac{1}{{\sigma_2}^2(-Q^2+3RP)}}(\frac{3}{2}\zeta-2\cos(\zeta)-\frac{1}{2}\sin(\zeta)\cos(\zeta))
\end{aligned}$$

$$- 2\sqrt[4]{-\frac{1}{\sigma_2{}^2(-Q^2+3RP)}}P(\zeta-\cos(\zeta))$$
$$+ \frac{1}{3\sigma_2}(1+3\sqrt{-\frac{1}{\sigma_2{}^2(-Q^2+3RP)}}\sigma_2 P + \sqrt{-\frac{1}{\sigma_2{}^2(-Q^2+3RP)}}\sigma_2 Q)\zeta\frac{1}{\sqrt[4]{-\frac{1}{\sigma_2{}^2(-Q^2+3RP)}}}\Big). \tag{4.22}$$

Family 1.6. For $R=1, \quad Q=2-4m^2, \quad P=1.$

Case 1. When $m\to 1$,

$$\begin{aligned}&\varphi_{1,17}(x,y,t)\\ =&e^{\rho\mathcal{B}(t)-\frac{\rho^2}{2}t}\Big(-\sqrt[4]{-\frac{1}{\sigma_2{}^2(-Q^2+3RP)}}\tanh(\zeta)-2\sqrt[4]{-\frac{1}{\sigma_2{}^2(-Q^2+3RP)}}\ln(\tanh(\zeta)-1)\\ &-\sqrt[4]{-\frac{1}{\sigma_2{}^2(-Q^2+3RP)}}P\zeta-2\sqrt[4]{-\frac{1}{\sigma_2{}^2(-Q^2+3RP)}}P\ln(\cosh(\zeta))+\frac{1}{3}\zeta\frac{1}{\sqrt[4]{-\frac{1}{\sigma_2{}^2(-Q^2+3RP)}}}\\ &+\frac{1}{3}\sqrt[4]{-\frac{1}{\sigma_2{}^2(-Q^2+3RP)}}\zeta Q\Big).\end{aligned} \tag{4.23}$$

Case 2. When $m\to 0$,

$$\begin{aligned}&\varphi_{1,18}(x,y,t)\\ =&e^{\rho\mathcal{B}(t)-\frac{\rho^2}{2}t}\Big(-2\sqrt[4]{-\frac{1}{\sigma_2{}^2(-Q^2+3RP)}}\ln(\cos(\zeta))+\sqrt[4]{-\frac{1}{\sigma_2{}^2(-Q^2+3RP)}}\tan(\zeta)\\ &-\sqrt[4]{-\frac{1}{\sigma_2{}^2(-Q^2+3\,RP)}}P\zeta+2\sqrt[4]{-\frac{1}{\sigma_2{}^2(-Q^2+3RP)}}P\ln(\cos(\zeta))+\frac{1}{3\sigma_2}\zeta\frac{1}{\sqrt[4]{-\frac{1}{\sigma_2{}^2(-Q^2+3RP)}}}\\ &+\frac{1}{3}\sqrt[4]{-\frac{1}{\sigma_2{}^2(-Q^2+3RP)}}\zeta\, Q\Big).\end{aligned} \tag{4.24}$$

Family 1.7. For $R=1, \quad Q=2, \quad P=m^2.$

Case 1. When $m\to 1$,

$$\begin{aligned}&\varphi_{1,19}(x,y,t)\\ =&e^{\rho\mathcal{B}(t)-\frac{\rho^2}{2}t}\Big(-\sqrt[4]{-\frac{1}{\sigma_2{}^2(-Q^2+3RP)}}\tanh(\zeta)-2\sqrt[4]{-\frac{1}{\sigma_2{}^2(-Q^2+3RP)}}\ln(\tanh(\zeta)-1)\\ &-\sqrt[4]{-\frac{1}{\sigma_2{}^2(-Q^2+3RP)}}P\zeta-2\sqrt[4]{-\frac{1}{\sigma_2{}^2(-Q^2+3RP)}}P\ln(\cosh(\zeta))+\frac{1}{3\sigma_2}\zeta\frac{1}{\sqrt[4]{-\frac{1}{\sigma_2{}^2(-Q^2+3RP)}}}\end{aligned}$$

$$+\frac{1}{3}\sqrt[4]{-\frac{1}{{\sigma_2}^2(-Q^2+3RP)}}\zeta Q\Big). \tag{4.25}$$

Case 2. When $m\to 0$,

$$\begin{aligned}&\varphi_{1,20}(x,y,t)\\ =&e^{\rho\mathcal{B}(t)-\frac{\rho^2}{2}t}\Big(\sqrt[4]{-\frac{1}{{\sigma_2}^2(-Q^2+3RP)}}(\frac{9}{8}\zeta-(\cos(\zeta))^2-\frac{1}{4}\sin(\zeta)(\cos(\zeta))^3+\frac{1}{8}\sin(\zeta)\cos(\zeta))\\ &-2\sqrt[4]{-\frac{1}{{\sigma_2}^2(-Q^2+3RP)}}P(\zeta-\frac{1}{2}(\cos(\zeta))^2)\\ &+\frac{1}{3\sigma_2}(1+3\sqrt{-\frac{1}{{\sigma_2}^2(-Q^2+3RP)}}\sigma_2P+\sqrt{-\frac{1}{{\sigma_2}^2(-Q^2+3RP)}}\sigma_2Q)\zeta\frac{1}{\sqrt[4]{-\frac{1}{{\sigma_2}^2(-Q^2+3RP)}}}\Big).\end{aligned} \tag{4.26}$$

Assuming the Case 2, we get the following families of solutions with the help of Table 1.

Family 2.1. For $R=1-m^2,\quad Q=2-m^2,\quad P=1.$

Case 1. When $m\to 1$,

$$\begin{aligned}&\varphi_{2,1}(x,y,t)\\ =&e^{\rho\mathcal{B}(t)-\frac{\rho^2}{2}t}\Big(\iota\sqrt[4]{-\frac{1}{{\sigma_2}^2(-Q^2+3RP)}}\zeta-4\iota\sqrt[4]{-\frac{1}{{\sigma_2}^2(-Q^2+3RP)}}\operatorname{arctanh}(e^{\zeta})\\ &-\iota\sqrt[4]{-\frac{1}{{\sigma_2}^2(-Q^2+3RP)}}\coth(\zeta)-i\sqrt[4]{-\frac{1}{{\sigma_2}^2(-Q^2+3RP)}}P\zeta-2\iota\sqrt[4]{-\frac{1}{{\sigma_2}^2(-Q^2+3RP)}}P\\ &\times\ln(\tanh(\frac{1}{2}\zeta))-\frac{1}{3\sigma_2}\iota\zeta\frac{1}{\sqrt[4]{-\frac{1}{{\sigma_2}^2(-Q^2+3RP)}}}+\frac{1}{3}\iota\sqrt[4]{-\frac{1}{{\sigma_2}^2(-Q^2+3RP)}}\zeta Q\Big).\end{aligned} \tag{4.27}$$

Case 2. When $m\to 0$,

$$\begin{aligned}&\varphi_{2,2}(x,y,t)\\ =&e^{\rho\mathcal{B}(t)-\frac{\rho^2}{2}t}\Big(-\iota\sqrt[4]{-\frac{1}{{\sigma_2}^2(-Q^2+3RP)}}\cot(\zeta)-\iota\sqrt[4]{-\frac{1}{{\sigma_2}^2(-Q^2+3RP)}}\ln(\csc^2(\zeta))\\ &-\iota\sqrt[4]{-\frac{1}{{\sigma_2}^2(-Q^2+3RP)}}P\zeta-2\iota\sqrt[4]{-\frac{1}{{\sigma_2}^2(-Q^2+3RP)}}P\\ &\times\ln(\sin(\zeta))-\frac{1}{3\sigma_2}\iota\zeta\frac{1}{\sqrt[4]{-\frac{1}{{\sigma_2}^2(-Q^2+3RP)}}}+\frac{1}{3}\iota\sqrt[4]{-\frac{1}{{\sigma_2}^2(-Q^2+3\,RP)}}\zeta Q\Big).\end{aligned} \tag{4.28}$$

Family 2.2. For $R=\frac{1}{4},\quad Q=\frac{1-2m^2}{2},\quad P=\frac{1}{4}.$

Case 1. When $m\to 1$,

$$\varphi_{2,3}(x,y,t)$$

$$
\begin{aligned}
=&e^{\rho\mathcal{B}(t)-\frac{\rho^2}{2}t}\Big(2\iota\sqrt[4]{-\frac{1}{{\sigma_2}^2(-Q^2+3RP)}}\zeta+2\,\iota\sqrt[4]{-\frac{1}{{\sigma_2}^2(-Q^2+3RP)}}\ln(\sinh(\zeta))\\
&-4\iota\sqrt[4]{-\frac{1}{{\sigma_2}^2(-Q^2+3RP)}}\operatorname{arctanh}(\mathrm{e}^{\zeta})-\iota\sqrt[4]{-\frac{1}{{\sigma_2}^2(-Q^2+3RP)}}\coth(\zeta)\\
&-2\iota\sqrt[4]{-\frac{1}{{\sigma_2}^2(-Q^2+3RP)}}\coth(\zeta)\operatorname{csch}(\zeta)+2\iota\sqrt[4]{-\frac{1}{{\sigma_2}^2(-Q^2+3RP)}}\sinh(\zeta)\\
&-\iota\sqrt[4]{-\frac{1}{{\sigma_2}^2(-Q^2+3RP)}}\coth(\zeta)-\iota\sqrt[4]{-\frac{1}{{\sigma_2}^2(-Q^2+3RP)}}P\zeta-2\iota\sqrt[4]{-\frac{1}{{\sigma_2}^2(-Q^2+3RP)}}P\\
&\times\ln(\sinh(\zeta))-2\iota\sqrt[4]{-\frac{1}{{\sigma_2}^2(-Q^2+3RP)}}P\ln(\tanh(\frac{1}{2}\zeta))-\frac{1}{3\sigma_2}\iota\zeta\frac{1}{\sqrt[4]{-\frac{1}{{\sigma_2}^2(-Q^2+3RP)}}}\\
&+\frac{1}{3}\iota\sqrt[4]{-\frac{1}{{\sigma_2}^2(-Q^2+3\,RP)}}\zeta Q\Big),
\end{aligned}
\tag{4.29}
$$

$$
\begin{aligned}
&\varphi_{2,4}(x,y,t)\\
=&e^{\rho\mathcal{B}(t)-\frac{\rho^2}{2}t}\Big(2\iota\sqrt[4]{-\frac{1}{{\sigma_2}^2(-Q^2+3RP)}}\zeta+2\,\iota\sqrt[4]{-\frac{1}{{\sigma_2}^2(-Q^2+3RP)}}\ln(\sinh(\zeta))\\
&+4\iota\sqrt[4]{-\frac{1}{{\sigma_2}^2(-Q^2+3RP)}}\operatorname{arctanh}(\mathrm{e}^{\zeta})-\iota\sqrt[4]{-\frac{1}{{\sigma_2}^2(-Q^2+3RP)}}\coth(\zeta)\\
&+2\iota\sqrt[4]{-\frac{1}{{\sigma_2}^2(-Q^2+3RP)}}\coth(\zeta)\operatorname{csch}(\zeta)-2\iota\sqrt[4]{-\frac{1}{{\sigma_2}^2(-Q^2+3RP)}}\sinh(\zeta)\\
&-\iota\sqrt[4]{-\frac{1}{{\sigma_2}^2(-Q^2+3RP)}}\coth(\zeta)-\iota\sqrt[4]{-\frac{1}{{\sigma_2}^2(-Q^2+3RP)}}P\zeta\\
&-2\iota\sqrt[4]{-\frac{1}{{\sigma_2}^2(-Q^2+3RP)}}P\ln(\sinh(\zeta))+2\iota\sqrt[4]{-\frac{1}{{\sigma_2}^2(-Q^2+3RP)}}P\\
&\times\ln(\tanh(\frac{1}{2}\zeta))-\frac{1}{3\sigma_2}\iota\zeta\frac{1}{\sqrt[4]{-\frac{1}{{\sigma_2}^2(-Q^2+3RP)}}}+\frac{1}{3}\iota\sqrt[4]{-\frac{1}{{\sigma_2}^2(-Q^2+3\,RP)}}\zeta Q\Big),
\end{aligned}
\tag{4.30}
$$

$$
\begin{aligned}
&\varphi_{2,5}(x,y,t)\\
=&e^{\rho\mathcal{B}(t)-\frac{\rho^2}{2}t}\Big(-2\iota\sqrt[4]{-\frac{1}{{\sigma_2}^2(-Q^2+3RP)}}\tanh(\frac{1}{2}\zeta)-4\iota\sqrt[4]{-\frac{1}{{\sigma_2}^2(-Q^2+3RP)}}\ln(\tanh(\frac{1}{2}\zeta)-1)\\
&-\iota\sqrt[4]{-\frac{1}{{\sigma_2}^2(-Q^2+3RP)}}P\zeta+2\iota\sqrt[4]{-\frac{1}{{\sigma_2}^2(-Q^2+3RP)}}P\ln(\operatorname{sech}(\zeta))\\
&-2\iota\sqrt[4]{-\frac{1}{{\sigma_2}^2(-Q^2+3RP)}}P\ln(1+\operatorname{sech}(\zeta))-\frac{1}{3\sigma_2}\iota\zeta\frac{1}{\sqrt[4]{-\frac{1}{{\sigma_2}^2(-Q^2+3RP)}}}
\end{aligned}
$$

$$+\frac{1}{3}\iota\sqrt[4]{-\frac{1}{{\sigma_2}^2(-Q^2+3\,RP)}}\zeta Q\Big), \tag{4.31}$$

$$\begin{aligned}&\varphi_{2,6}(x,y,t)\\ =&e^{\rho\mathcal{B}(t)-\frac{\rho^2}{2}t}\Big(4\iota\sqrt[4]{-\frac{1}{{\sigma_2}^2(-Q^2+3RP)}}\ln(\tanh(\frac{1}{2}\zeta))-4\iota\sqrt[4]{-\frac{1}{{\sigma_2}^2(-Q^2+3RP)}}\ln(\tanh(\frac{1}{2}\zeta)-1)\\ &-2\iota\sqrt[4]{-\frac{1}{{\sigma_2}^2(-Q^2+3RP)}}\coth(\frac{1}{2}\zeta)-\iota\sqrt[4]{-\frac{1}{{\sigma_2}^2(-Q^2+3RP)}}P\zeta+2\iota\sqrt[4]{-\frac{1}{{\sigma_2}^2(-Q^2+3RP)}}P\\ &\times\ln(\mathrm{sech}(\zeta))-2\iota\sqrt[4]{-\frac{1}{{\sigma_2}^2(-Q^2+3RP)}}P\ln(-1+\mathrm{sech}(\zeta))-\frac{1}{3\sigma_2}\iota\zeta\frac{1}{\sqrt[4]{-\frac{1}{{\sigma_2}^2(-Q^2+3RP)}}}\\ &+\frac{1}{3}\iota\sqrt[4]{-\frac{1}{{\sigma_2}^2(-Q^2+3RP)}}\zeta Q\Big).\end{aligned} \tag{4.32}$$

Case 2. When $m\to 0$,

$$\begin{aligned}&\varphi_{2,7}(x,y,t)\\ =&e^{\rho\mathcal{B}(t)-\frac{\rho^2}{2}t}\Big(2\iota\sqrt[4]{-\frac{1}{{\sigma_2}^2(-Q^2+3RP)}}\ln(\sec(\zeta)+\tan(\zeta))+2\iota\sqrt[4]{-\frac{1}{{\sigma_2}^2(-Q^2+3RP)}}\ln(\sin(\zeta))\\ &+i\ sqrt[4]-\frac{1}{{\sigma_2}^2(-Q^2+3RP)}\tan(\zeta)+2\iota\sqrt[4]{-\frac{1}{{\sigma_2}^2(-Q^2+3RP)}}\ln(\csc(\zeta)-\cot(\zeta))\\ &-\iota\sqrt[4]{-\frac{1}{{\sigma_2}^2(-Q^2+3RP)}}\cot(\zeta)-\iota\sqrt[4]{-\frac{1}{{\sigma_2}^2(-Q^2+3RP)}}P\zeta-2\iota\sqrt[4]{-\frac{1}{{\sigma_2}^2(-Q^2+3RP)}}P\\ &\times\ln(\sec(\zeta)+\tan(\zeta))-2\iota\sqrt[4]{-\frac{1}{{\sigma_2}^2(-Q^2+3RP)}}P\ln(\sin(\zeta))-\frac{1}{3\sigma_2}\iota\zeta\frac{1}{\sqrt[4]{-\frac{1}{{\sigma_2}^2(-Q^2+3\,RP)}}}\\ &+\frac{1}{3}\iota\sqrt[4]{-\frac{1}{{\sigma_2}^2(-Q^2+3RP)}}\zeta Q\Big),\end{aligned} \tag{4.33}$$

$$\begin{aligned}&\varphi_{2,8}(x,y,t)\\ =&e^{\rho\mathcal{B}(t)-\frac{\rho^2}{2}t}\Big(2\iota\sqrt[4]{-\frac{1}{{\sigma_2}^2(-Q^2+3RP)}}\ln(\sec(\zeta)+\tan(\zeta))-2\,\iota\sqrt[4]{-\frac{1}{{\sigma_2}^2(-Q^2+3RP)}}\ln(\sin(\zeta))\\ &+\iota\sqrt[4]{-\frac{1}{{\sigma_2}^2(-Q^2+3RP)}}\tan(\zeta)-2\,\iota\sqrt[4]{-\frac{1}{{\sigma_2}^2(-Q^2+3RP)}}\ln(\csc(\zeta)-\cot(\zeta))\\ &-\iota\sqrt[4]{-\frac{1}{{\sigma_2}^2(-Q^2+3RP)}}\cot(\zeta)-\iota\sqrt[4]{-\frac{1}{{\sigma_2}^2(-Q^2+3RP)}}P\zeta-2\iota\sqrt[4]{-\frac{1}{{\sigma_2}^2(-Q^2+3RP)}}P\\ &\times\ln(\sec(\zeta)+\tan(\zeta))+2\iota\sqrt[4]{-\frac{1}{{\sigma_2}^2(-Q^2+3RP)}}P\ln(\sin(\zeta))-\frac{1}{3\sigma_2}\iota\zeta\frac{1}{\sqrt[4]{-\frac{1}{{\sigma_2}^2(-Q^2+3\,RP)}}}\end{aligned}$$

$$+\frac{1}{3}\iota\sqrt[4]{-\frac{1}{{\sigma_2}^2(-Q^2+3RP)}}\zeta Q\Big), \tag{4.34}$$

$$\begin{aligned}
&\varphi_{2,9}(x,y,t)\\
=&e^{\rho\mathcal{B}(t)-\frac{\rho^2}{2}t}\Big(2\iota\sqrt[4]{-\frac{1}{{\sigma_2}^2(-Q^2+3RP)}}\tan(\frac{1}{2}\zeta)+2\iota\sqrt[4]{-\frac{1}{{\sigma_2}^2(-Q^2+3RP)}}\ln((\tan(\frac{1}{2}\zeta))^2+1)\\
&-\iota\sqrt[4]{-\frac{1}{{\sigma_2}^2(-Q^2+3RP)}}P\zeta+2\iota\sqrt[4]{-\frac{1}{{\sigma_2}^2(-Q^2+3RP)}}P\ln(1+\cos(\zeta))\\
&-\frac{1}{3\sigma_2}\iota\zeta\frac{1}{\sqrt[4]{-\frac{1}{{\sigma_2}^2(-Q^2+3RP)}}}+\frac{1}{3}\iota\sqrt[4]{-\frac{1}{{\sigma_2}^2(-Q^2+3RP)}}\zeta Q\Big),
\end{aligned} \tag{4.35}$$

$$\begin{aligned}
&\varphi_{2,10}(x,y,t)\\
=&e^{\rho\mathcal{B}(t)-\frac{\rho^2}{2}t}\Big(-2\iota\sqrt[4]{-\frac{1}{{\sigma_2}^2(-Q^2+3RP)}}\ln((\tan(\frac{1}{2}\zeta))^2+1)\\
&-2\iota\sqrt[4]{-\frac{1}{{\sigma_2}^2(-Q^2+3RP)}}(\tan(\frac{1}{2}\zeta))^{-1}+4\iota\sqrt[4]{-\frac{1}{{\sigma_2}^2(-Q^2+3RP)}}\ln(\tan(\frac{1}{2}\zeta))\\
&-\iota\sqrt[4]{-\frac{1}{{\sigma_2}^2(-Q^2+3RP)}}P\zeta-2\iota\sqrt[4]{-\frac{1}{{\sigma_2}^2(-Q^2+3RP)}}P\ln(1-\cos(\zeta))\\
&-\frac{1}{3\sigma_2}\iota\zeta\frac{1}{\sqrt[4]{-\frac{1}{{\sigma_2}^2(-Q^2+3\,RP)}}}+\frac{1}{3}\iota\sqrt[4]{-\frac{1}{{\sigma_2}^2(-Q^2+3RP)}}\zeta Q\Big).
\end{aligned} \tag{4.36}$$

Family 2.3. For $R=\frac{1-m^2}{4}$, $\quad Q=\frac{1+m^2}{2}$, $\quad P=\frac{1-m^2}{4}$.

Case 1. When $m\to 1$,

$$\begin{aligned}
&\varphi_{2,11}(x,y,t)\\
=&e^{\rho\mathcal{B}(t)-\frac{\rho^2}{2}t}\Big(\iota\sqrt[4]{-\frac{1}{{\sigma_2}^2(-Q^2+3RP)}}(\zeta+2\,\sinh(\zeta)+2\,\cosh(\zeta)+\cosh(\zeta)\sinh(\zeta)+(\cosh(\zeta))^2)\\
&-2\iota\sqrt[4]{-\frac{1}{{\sigma_2}^2(-Q^2+3RP)}}P(\zeta+\sinh(\zeta)+\cosh(\zeta))\\
&+\frac{1}{3\sigma_2}i(-1+3\sqrt{-\frac{1}{{\sigma_2}^2(-Q^2+3RP)}}\sigma_2P+\sqrt{-\frac{1}{{\sigma_2}^2(-Q^2+3\,RP)}}\sigma_2Q)\zeta\frac{1}{\sqrt[4]{-\frac{1}{{\sigma_2}^2(-Q^2+3RP)}}}\Big).
\end{aligned} \tag{4.37}$$

Case 2. When $m\to 0$,

$$\begin{aligned}
&\varphi_{2,12}(x,y,t)\\
=&e^{\rho\mathcal{B}(t)-\frac{\rho^2}{2}t}\Big(\iota\sqrt[4]{-\frac{1}{{\sigma_2}^2(-Q^2+3RP)}}\tan(\zeta)+2\,\iota\sqrt[4]{-\frac{1}{{\sigma_2}^2(-Q^2+3RP)}}\ln(\sec(\zeta)+\tan(\zeta))
\end{aligned}$$

$$+ 2\iota \sqrt[4]{-\frac{1}{{\sigma_2}^2(-Q^2+3RP)}}\sec(\zeta) - 2\iota \sqrt[4]{-\frac{1}{{\sigma_2}^2(-Q^2+3RP)}}\ln(\cos(\zeta))$$

$$+ \iota \sqrt[4]{-\frac{1}{{\sigma_2}^2(-Q^2+3RP)}}\tan(\zeta) - \iota \sqrt[4]{-\frac{1}{{\sigma_2}^2(-Q^2+3RP)}}P\zeta - 2\iota \sqrt[4]{-\frac{1}{{\sigma_2}^2(-Q^2+3RP)}}P$$

$$\times \ln(\sec(\zeta)+\tan(\zeta)) + 2\iota \sqrt[4]{-\frac{1}{{\sigma_2}^2(-Q^2+3RP)}}P\ln(\cos(\zeta))$$

$$- \frac{1}{3\sigma_2}\iota\zeta\frac{1}{\sqrt[4]{-\frac{1}{{\sigma_2}^2(-Q^2+3RP)}}} + \frac{1}{3}\iota \sqrt[4]{-\frac{1}{{\sigma_2}^2(-Q^2+3RP)}}\zeta Q\Big). \tag{4.38}$$

Family 2.4. For $R = 1, \quad Q = 2 - m^2, \quad P = 1 - m^2$.

Case 1. When $m \to 1$,

$$\begin{aligned}&\varphi_{2,13}(x,y,t)\\ =&e^{\rho\mathcal{B}(t)-\frac{\rho^2}{2}t}\Big(\iota \sqrt[4]{-\frac{1}{{\sigma_2}^2(-Q^2+3RP)}}(\frac{1}{2}\zeta + 2\,\cosh(\zeta) + \frac{1}{2}\cosh(\zeta)\sinh(\zeta))\\ &- 2\iota \sqrt[4]{-\frac{1}{{\sigma_2}^2(-Q^2+3RP)}}P(\zeta+\cosh(\zeta)) + \frac{1}{3\sigma_2}i(-1+3\sqrt{-\frac{1}{{\sigma_2}^2(-Q^2+3RP)}}\sigma_2 P\\ &+ \sqrt{-\frac{1}{{\sigma_2}^2(-Q^2+3RP)}}\sigma_2 Q)\zeta\frac{1}{\sqrt[4]{-\frac{1}{{\sigma_2}^2(-Q^2+3RP)}}}\Big).\end{aligned} \tag{4.39}$$

Case 2. When $m \to 0$,

$$\begin{aligned}&\varphi_{2,14}(x,y,t)\\ =&e^{\rho\mathcal{B}(t)-\frac{\rho^2}{2}t}\Big(\iota \sqrt[4]{-\frac{1}{{\sigma_2}^2(-Q^2+3RP)}}\tan(\zeta) + \iota \sqrt[4]{-\frac{1}{{\sigma_2}^2(-Q^2+3RP)}}\ln(\sec^2(\zeta))\\ &- \iota \sqrt[4]{-\frac{1}{{\sigma_2}^2(-Q^2+3RP)}}P\zeta + 2\iota \sqrt[4]{-\frac{1}{{\sigma_2}^2(-Q^2+3RP)}}P\ln(\cos(\zeta)) - \frac{1}{3\sigma_2}\iota\zeta\frac{1}{\sqrt[4]{-\frac{1}{{\sigma_2}^2(-Q^2+3RP)}}}\\ &+ \frac{1}{3}\iota \sqrt[4]{-\frac{1}{{\sigma_2}^2(-Q^2+3\,RP)}}\zeta Q\Big).\end{aligned} \tag{4.40}$$

Family 2.5. For $R = 1, \quad Q = 2m^2 - 1, \quad P = -m(1 - m^2)$.

Case 1. When $m \to 1$,

$$\begin{aligned}&\varphi_{2,15}(x,y,t)\\ =&e^{\rho\mathcal{B}(t)-\frac{\rho^2}{2}t}\Big(\iota \sqrt[4]{-\frac{1}{{\sigma_2}^2(-Q^2+3RP)}}(\frac{1}{2}\zeta + 2\,\cosh(\zeta) + \frac{1}{2}\cosh(\zeta)\sinh(\zeta))\end{aligned}$$

$$- 2\iota\sqrt[4]{-\frac{1}{{\sigma_2}^2(-Q^2+3RP)}}P(\zeta+\cosh(\zeta)) + \frac{1}{3\sigma_2}i(-1+3\sqrt{-\frac{1}{{\sigma_2}^2(-Q^2+3RP)}}\sigma_2 P + \sqrt{-\frac{1}{{\sigma_2}^2(-Q^2+3RP)}}\sigma_2 Q)\zeta\frac{1}{\sqrt[4]{-\frac{1}{{\sigma_2}^2(-Q^2+3RP)}}}\Big). \tag{4.41}$$

Case 2. When $m \to 0$,

$$\varphi_{2,16}(x,y,t) = e^{\rho\mathcal{B}(t)-\frac{\rho^2}{2}t}\Big(\iota\sqrt[4]{-\frac{1}{{\sigma_2}^2(-Q^2+3RP)}}(\frac{3}{2}\zeta - 2\cos(\zeta) - \frac{1}{2}\sin(\zeta)\cos(\zeta)) - 2\iota\sqrt[4]{-\frac{1}{{\sigma_2}^2(-Q^2+3RP)}}P(\zeta-\cos(\zeta)) + \frac{1}{3\sigma_2}\iota(-1+3\sqrt{-\frac{1}{{\sigma_2}^2(-Q^2+3RP)}}\sigma_2 P + \sqrt{-\frac{1}{{\sigma_2}^2(-Q^2+3RP)}}\sigma_2 Q)\zeta\frac{1}{\sqrt[4]{-\frac{1}{{\sigma_2}^2(-Q^2+3RP)}}}\Big). \tag{4.42}$$

Family 2.6. For $R = 1, \quad Q = 2-4m^2, \quad P = 1.$

Case 1. When $m \to 1$,

$$\varphi_{2,17}(x,y,t) = e^{\rho\mathcal{B}(t)-\frac{\rho^2}{2}t}\Big(-\iota\sqrt[4]{-\frac{1}{{\sigma_2}^2(-Q^2+3RP)}}\tanh(\zeta) - 2\iota\sqrt[4]{-\frac{1}{{\sigma_2}^2(-Q^2+3RP)}}\ln(\tanh(\zeta)-1) - \iota\sqrt[4]{-\frac{1}{{\sigma_2}^2(-Q^2+3RP)}}P\zeta - 2\iota\sqrt[4]{-\frac{1}{{\sigma_2}^2(-Q^2+3RP)}}P\ln(\cosh(\zeta)) - \frac{1}{3\sigma_2}\iota\zeta\frac{1}{\sqrt[4]{-\frac{1}{{\sigma_2}^2(-Q^2+3RP)}}} + \frac{1}{3}\iota\sqrt[4]{-\frac{1}{{\sigma_2}^2(-Q^2+3RP)}}\zeta Q\Big). \tag{4.43}$$

Case 2. When $m \to 0$,

$$\varphi_{2,18}(x,y,t) = e^{\rho\mathcal{B}(t)-\frac{\rho^2}{2}t}\Big(-2\iota\sqrt[4]{-\frac{1}{{\sigma_2}^2(-Q^2+3RP)}}\ln(\cos(\zeta)) + \iota\sqrt[4]{-\frac{1}{{\sigma_2}^2(-Q^2+3RP)}}\tan(\zeta) - \iota\sqrt[4]{-\frac{1}{{\sigma_2}^2(-Q^2+3\,RP)}}P\zeta + 2\iota\sqrt[4]{-\frac{1}{{\sigma_2}^2(-Q^2+3RP)}}P\ln(\cos(\zeta)) - \frac{1}{3\sigma_2}\iota\zeta\frac{1}{\sqrt[4]{-\frac{1}{{\sigma_2}^2(-Q^2+3RP)}}} + \frac{1}{3}\iota\sqrt[4]{-\frac{1}{{\sigma_2}^2(-Q^2+3RP)}}\zeta Q\Big). \tag{4.44}$$

Family. 2.7. For $R = 1, \quad Q = 2, \quad P = m^2$.

Case 1. When $m \to 1$,

$$
\begin{aligned}
&\varphi_{2,19}(x,y,t)\\
=&e^{\rho\mathcal{B}(t)-\frac{\rho^2}{2}t}\Big(-\iota\sqrt[4]{-\frac{1}{{\sigma_2}^2(-Q^2+3RP)}}\tanh(\zeta) - 2\iota\sqrt[4]{-\frac{1}{{\sigma_2}^2(-Q^2+3RP)}}\ln(\tanh(\zeta)-1)\\
&-\iota\sqrt[4]{-\frac{1}{{\sigma_2}^2(-Q^2+3RP)}}P\zeta - 2\iota\sqrt[4]{-\frac{1}{{\sigma_2}^2(-Q^2+3RP)}}P\ln(\cosh(\zeta))\\
&-\frac{1}{3\sigma_2}\iota\zeta\frac{1}{\sqrt[4]{-\frac{1}{{\sigma_2}^2(-Q^2+3RP)}}} + \frac{1}{3}\iota\sqrt[4]{-\frac{1}{{\sigma_2}^2(-Q^2+3RP)}}\zeta Q\Big).
\end{aligned} \tag{4.45}
$$

Case 2. When $m \to 0$,

$$
\begin{aligned}
&\varphi_{2,20}(x,y,t)\\
=&e^{\rho\mathcal{B}(t)-\frac{\rho^2}{2}t}\Big(\iota\sqrt[4]{-\frac{1}{{\sigma_2}^2(-Q^2+3RP)}}(\frac{9}{8}\zeta-(\cos(\zeta))^2-\frac{1}{4}\sin(\zeta)(\cos(\zeta))^3+\frac{1}{8}\sin(\zeta)\cos(\zeta))\\
&-2\iota\sqrt[4]{-\frac{1}{{\sigma_2}^2(-Q^2+3RP)}}P(\zeta-\frac{1}{2}(\cos(\zeta))^2)\\
&+\frac{1}{3\sigma_2}\iota(-1+3\sqrt{-\frac{1}{{\sigma_2}^2(-Q^2+3RP)}}\sigma_2P+\sqrt{-\frac{1}{{\sigma_2}^2(-Q^2+3RP)}}\sigma_2Q)\zeta\frac{1}{\sqrt[4]{-\frac{1}{{\sigma_2}^2(-Q^2+3RP)}}}\Big).
\end{aligned} \tag{4.46}
$$

5. Discussion and graphs

This fragment presents a graphical analysis of some solutions in $3D$ and contour forms, which are attained above and are different from those in the available literature. We plot some solutions for example, $|\varphi_{2,1}(x,y,t)|$, $|\varphi_{2,5}(x,y,t)|$, $|\varphi_{2,8}(x,y,t)|$, $|\varphi_{2,10}(x,y,t)|$, $|\varphi_{2,11}(x,y,t)|$, $|\varphi_{2,12}(x,y,t)|$, $|\varphi_{2,17}(x,y,t)|$, $|\varphi_{2,18}(x,y,t)|$ and $|\varphi_{2,20}(x,y,t)|$ by giving them specific values to pre-parameters mentioned in each case with the help of Maple software. The Figures 1-9 produces different dark soliton solutions of the considered system.

In all these figures, it can be observed that when the noise term is ignored (i.e $\rho = 0$), we see from Figures 1, 2, 3 and Figures 7, 8, 9, that there are some fluctuations and are not totally flat, but when the noise term is included, (i.e. $\rho = 2.5$), the surfaces after minor transit changes their shapes to more planar, and the periodicity has been reduced. Also in Figures 4, 5, 6, it can be seen that their shapes are changed after including the noise term. This shows that the stochastic term has some effects on the solutions of the considered interaction system and stabilizes the solutions around zero.

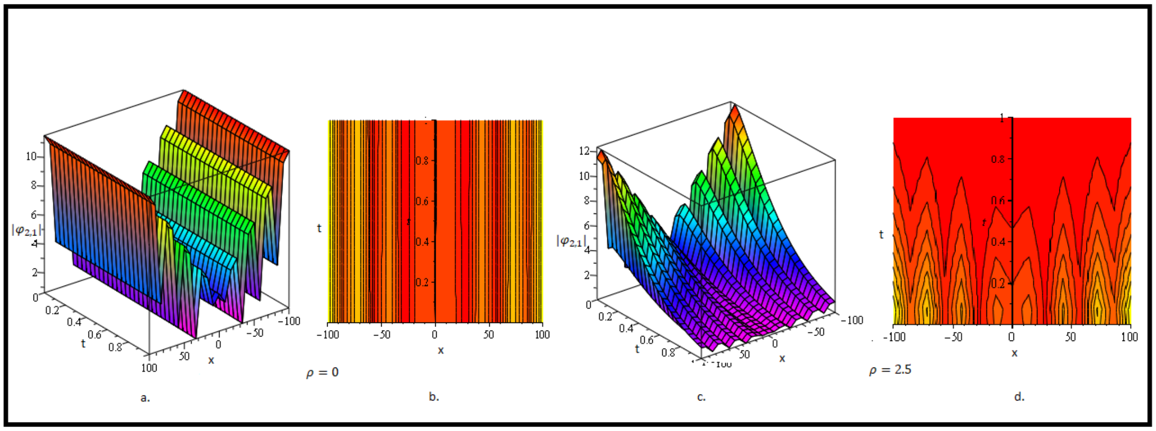

Figure 1. The 3D and contour graphs representing $|\varphi_{2,1}(x,y,t)|$ with and without resonance given in (4.27) for the values $m = .999999991$, $\sigma_2 = (1+\iota)^4$, $\beta = 1$, $\alpha = 1$, $y = 1$.

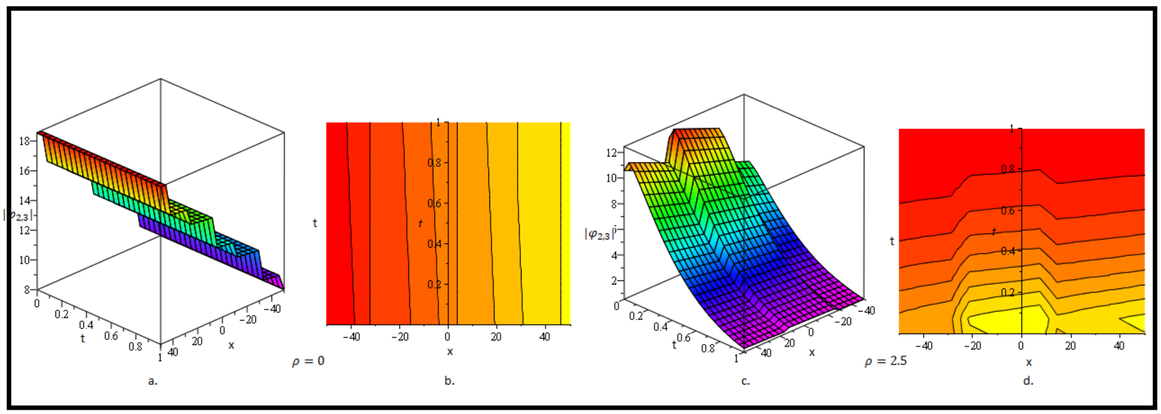

Figure 2. The 3D and contour graphs representing $|\varphi_{2,5}(x,y,t)|$ with and without resonance given in (4.31) for the values $m = .9999999999999999999999991$, $\sigma_2 = (1+2\iota)^4$, $\beta = 1$, $\alpha = 1$, $y = 1$.

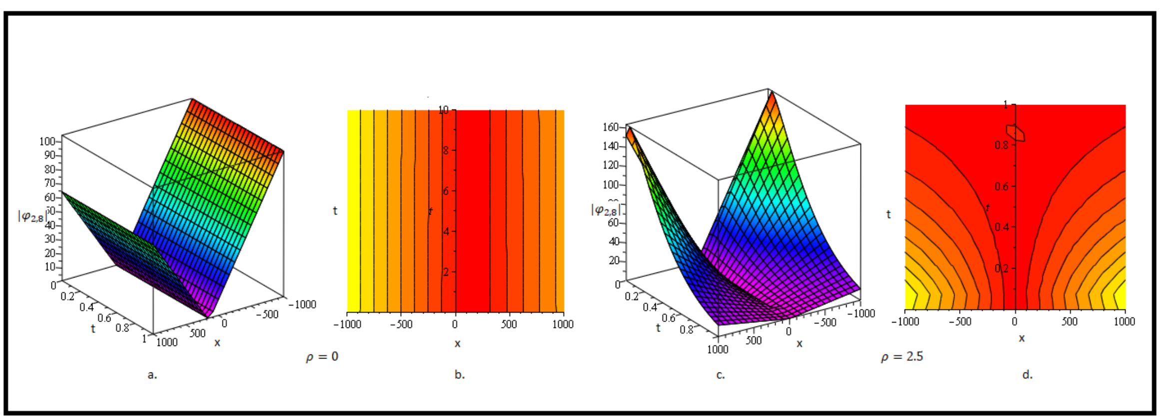

Figure 3. The 3D graphs representing $|\varphi_{2,8}(x,y,t)|$ with and without resonance given in (4.34) for the values $m = 0.00001$, $\sigma_2 = (1+2\iota)^4$, $\beta = 1$, $\alpha = 1$, $y = 1$.

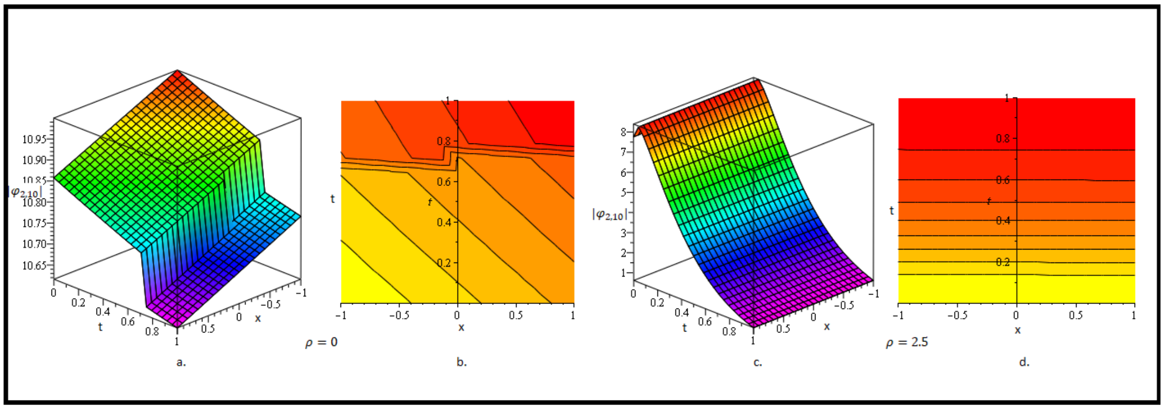

Figure 4. The 3D and contour graphs representing $|\varphi_{2,10}(x, y, t)|$ with and without resonance given in (4.36) for the values $m = 0.1e - 11$, $\sigma_2 = (1 + 2\iota)^4$, $\beta = 1$, $\alpha = 1$, $y = 1$.

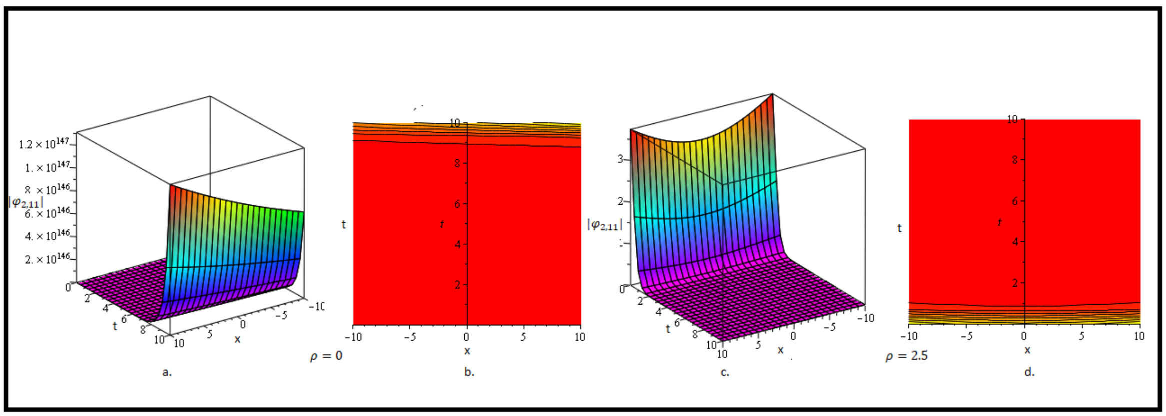

Figure 5. The 3D and contour graphs representing $|\varphi_{2,11}(x, y, t)|$ with and without resonance given in (4.37) for the values $m = .9999999999999991$, $S_{-2} = (1 - 4\iota)^4$, $\beta = 1$, $\alpha = 1$, $y = 1$.

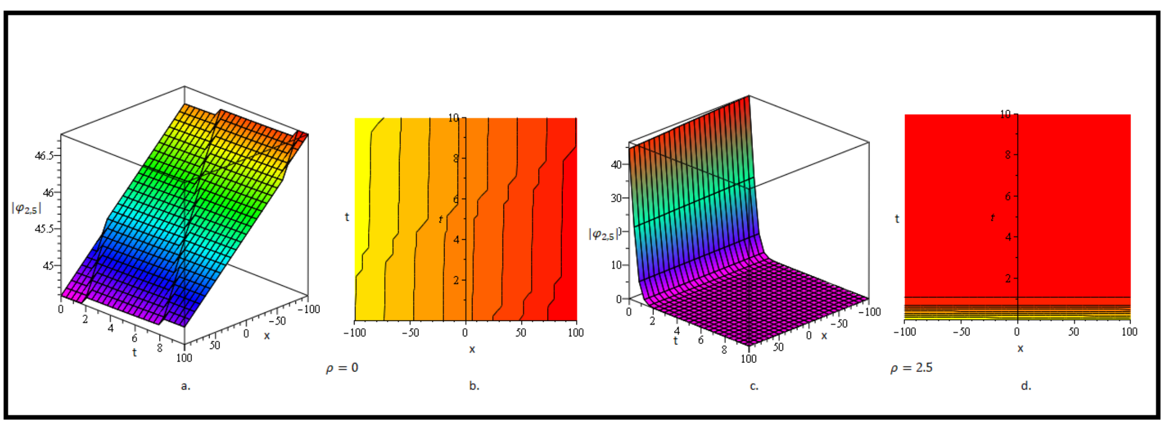

Figure 6. The 3D and contour graphs representing $|\varphi_{2,12}(x, y, t)|$ with and without resonance given in (4.38) for the values $m = 0.1e - 16$, $\sigma_2 = (1 + 4\iota)^4$, $\beta = 1$, $\alpha = 1$, $y = 1$.

Remark 5.1. In all of the above cases

$$\zeta = \frac{\Gamma(\beta + 1)}{\alpha}\Big(\sigma_1 x^\alpha + \sigma_2 y^\alpha\Big) + t.$$

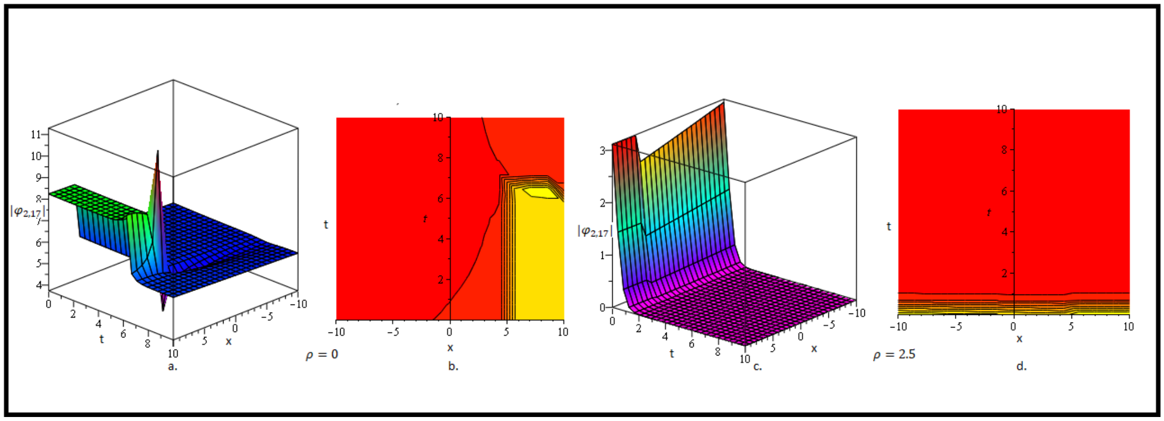

Figure 7. The 3D and contour graphs representing $|\varphi_{2,17}(x, y, t)|$ with and without resonance given in (4.43) for the values $m = .9999999999999999999999991$, $\sigma_2 = (1 + 2\iota)^4$, $\beta = 1$, $\alpha = 1$, $y = 1$.

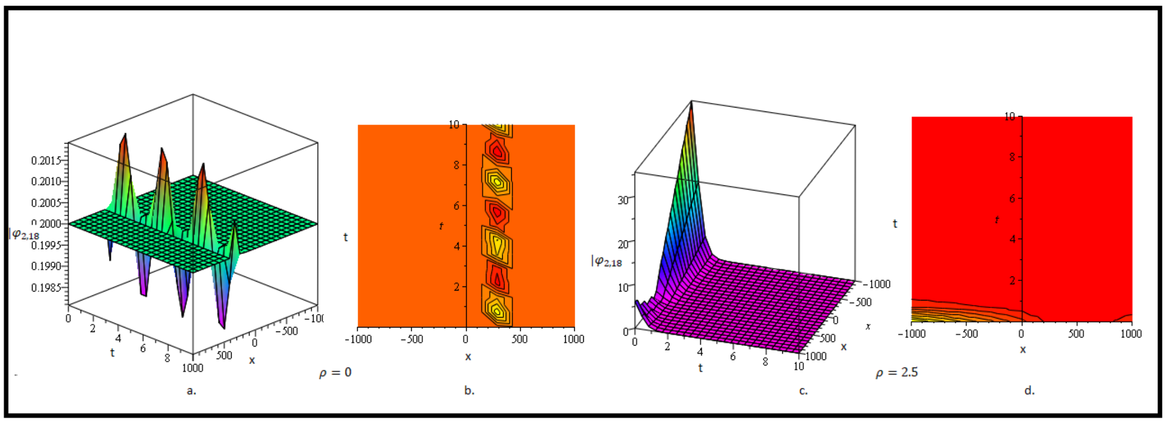

Figure 8. The 3D and contour graphs representing $|\varphi_{2,18}(x, y, t)|$ with and without resonance given in (4.44) for the values $m = 0.1e - 11$, $\sigma_2 = (1 + \iota)^4$, $\beta = 1$, $\alpha = 1$, $y = 1$.

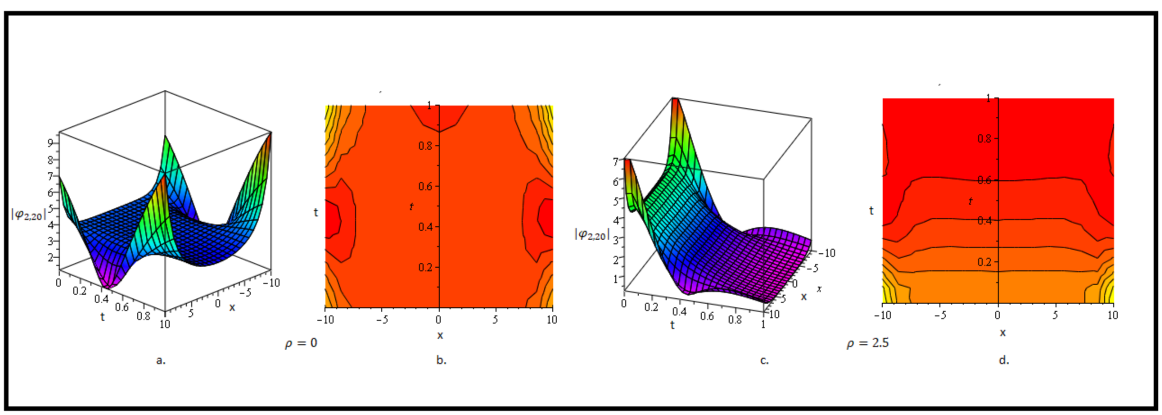

Figure 9. The 3D and contour graphs representing $|\varphi_{2,20}(x, y, t)|$ with and without resonance given in (4.46) for the values $m = 0.1e - 11$, $\sigma_2 = (1 + \iota)^4$, $\beta = 1$, $\alpha = 1$, $y = 1$.

6. Conclusion

In this study, we derived analytical stochastic fractional space-time solutions of system (1.1) in the form of trigonometric and hyperbolic functions. Using the GKAJM, we obtained exact solutions that can describe a range of complex physical phenomena in plasma physics, gravitation, nonlinear optics, biophysics, and water wave dynamics. Furthermore, Maple was used to generate graphical illustrations demonstrating the influence of multiplicative Bm on the solutions of (1.1), revealing that the noise term contributes to stabilizing the system's dynamics. Overall, our findings confirm that GKAJM is an effective analytical tool for solving nonlinear fractional SPDEs and for uncovering new families of exact solutions. The method is well-suited for analyzing time-fractional dispersive long-wave equations and nonlinear stochastic systems such as the fractional space-time stochastic breaking soliton equation FSTSBSE.

Data availability statement. No new data is generated.

Conflict of interest. None declared.

Acknowledgments. The authors would like to thank the editors and reviewers for their constructive feedback, which improved the presentation of the paper greatly.

Funding. No special funding is received.

Ethical statement. This article contains no studies with human participants or animals performed by the authors.

References

[1] M. A. Akbar, N. H. M. Ali and S. T. Mohyud-Din, *Assessment of the further improved* (G'/G)*-expansion method and the extended* tanh*-method in probing exact solutions of nonlinear PDEs*, Springer Plus, 2013, 2, 326.

[2] A. L. Alaoui, A. Elsonbaty, Y. Sabbar, M. Moumni and W. Adel, *Exploring stability characteristics of the Landau–Lifshitz–Bloch equation*, Partial Differential Equations in Applied Mathematics, 2024, 9, 100636.

[3] U. Ali, A. H Ganie, I. Khan, F. Alotaibi, K. Kamran, S. Muhammad and O. A. Al-Hartomy, *Traveling wave solutions to a mathematical model of fractional order* $(2+1)$*-dimensional breaking soliton equation*, Fractals., 2022, 30(5), 2240124.

[4] K. Ayub, M. Y. Khan and Q. Mahmood-Ul-Hassan, *Solitary and periodic wave solutions of Calogero-Bogoyavlenskii-Schiff equation via exp-function methods*, Computers and Mathematics with Applications, 2017, 74, 3231–3241.

[5] E. Barkai, R. Metzler and J. Klafter, *From continuous time random walks to the fractional Fokker–Planck equation*, Phys. Rev., 2000, 61, 1–8.

[6] A. Bekir, *Exact solutions for some* $(2+1)$*-dimensional nonlinear evolution equations by using the* tanh–coth *method*, World Appl. Sci. J., 2010, 9, 1–6.

[7] D. A. Benson, S. W. Wheatcraft and M. M. Meerschaert, *The fractional-order governing equation of Lévy motion*, Water Resour. Res., 2000, 36, 1413–1423.

[8] V. Capasso and D. Morale, *Stochastic modelling of tumour-induced angiogenesis*, J. Math. Biol., 2009, 58, 9–33.

[9] S. B. Chen, H. Ahanshahi, O. A. Abba, J. E. Olís-Pérez, S. Bekiros, J. F. Gómez-Aguilar, et al., *The effect of market confidence on a financial system from the perspective of fractional calculus: Numerical investigation and circuit realization*, Chaos Solitons Fractals, 2020, 140, 110223.

[10] S. B. Chen, S. Soradi-Zeid, H. Jahanshahi, R. Alcaraz, J. F. Gómez-Aguilar, S. Bekiros, et al., *Optimal control of time-delay fractional equations via a joint application of radial basis functions and collocation method*, Entropy, 2020, 22(11), 1213.

[11] Y. Chen and S. Ma, *Non-traveling wave solutions for the* (2+1)*-dimensional breaking soliton system*, Appl. Math., 2012, 3, 813–818.

[12] M. T. Darvishi and M. Najafi, *Some exact solutions of the* $(2+1)$*-dimensional breaking soliton equation using the three-wave method*, Int. J. Math. Comput. Sci., 2012, 87, 31–34.

[13] A. S. Devi, P. A. Naik, S. Boulaaras, N. Sene and Z. Huang, *Understanding the transmission mechanism of HIV/TB co-infection using fractional framework with optimal control*, International Journal of Numerical Modelling Electronic Networks Devices and Fields, 2025, 38(4), e70097.

[14] A. Ebaid and E. H. Aly, *Exact solutions for the transformed reduced Ostrovsky equation via the F-expansion method in terms of Weierstrass-elliptic and Jacobian-elliptic functions*, Wave Motion, 2012, 49, 296–308.

[15] M. Ekici, et al., *Optical solitons in birefringent fibers with Kerr nonlinearity by exp-function method*, Optik, 2017, 131, 964–976.

[16] A. A. Gaber, et al., *The generalized version of Kudryashov method for nonlinear space-time fractional partial differential equations of Burgers type*, Nonlinear Dynamics, 2019, 95, 361–368.

[17] A. H. Ganie, M. S. Rahaman, F. A. Aladsani and M. S. Ullah, *Bifurcation, chaos, and soliton analysis of the Manakov equation*, Nonlinear Dynamics, 2025, 113(9), 9807–9821.

[18] R. Gorenflo and F. Mainardi, *Random walk models for space-fractional diffusion processes*, Fract. Calc. Appl. Anal., 1998, 1, 167–191.

[19] B. Guo and D. Huang, *3D stochastic primitive equations of the large-scale ocean: Global well-posedness and attractors*, Comm. Math. Phys., 2009, 286, 697–723.

[20] M. Han, *Bifurcation Theory of Limit Cycles*, Science Press, Beijing, 2013.

[21] J. H. He and M. A. Abdou, *New periodic solutions for non-linear evolution equations using exp-function method*, Chaos, Solitons and Fractals, 2007, 34, 1421–1429.

[22] K. Hosseini, A. Bekir and R. Ansari, *New exact solutions of the conformable time-fractional Cahn–Allen and Cahn–Hilliard equations using the modified Kudryashov method*, Optik, 2017, 132, 203–209.

[23] G. Hu, Y. Lou and P. D. Christodes, *Dynamic output feedback covariance control of stochastic dissipative partial differential equations*, Chem. Eng. Sci., 2008, 63, 4531–4542.

[24] O. P. Ilhan and J. Manafian, *Periodic type and periodic cross-kink wave solutions to the* $(2+1)$*-dimensional breaking soliton equation arising in fluid dynamics*, Mod. Phys. Lett., 2019, 33, 1950277.

[25] S. M. Imran, S. Asghar and M. Mushtaq, *Mixed convection flow over an unsteady stretching surface in a porous medium with heat source*, Mathematical Problems in Engineering, 2012. DOI: 10.1155/2012/485418.

[26] N. Iqbal, R. Wu and W. W. Mohammed, *Pattern formation induced by fractional cross-diffusion in a 3-species food chain model with harvesting*, Math. Comput. Simulation, 2021, 188, 102–119.

[27] N. Iqbal, H. Yasmin, A. Ali, A. Bariq, M. M. Al-Sawalha and W. W. Mohammed, *Numerical methods for fractional-order Fornberg–Whitham equations in the sense of Atangana–Baleanu derivative*, J. Funct. Spaces, 2021, 2197247.

[28] H. Jahanshahi, D. Chen, Y.-M. Chu, J. F. Gómez-Aguilar and A. A. Aly, *Enhancement of the performance of nonlinear vibration energy harvesters by exploiting secondary resonances in multi-frequency excitations*, Eur. Phys. J. Plus, 2021, 136, 1–22.

[29] H. Jahanshahi, O. Orozco-López, J. M. Munoz-Pacheco, N. D. Alotaibi, C. Volos, Z. Wang, et al., *Simulation and experimental validation of a non-equilibrium chaotic system*, Chaos Solitons Fractals, 2021, 143, 110539.

[30] H. Joshi and B. K. Jha, *2D memory-based mathematical analysis for the combined impact of calcium influx and efflux on nerve cells*, Computers & Mathematics with Applications, 2023, 134, 33–44.

[31] H. Joshi and M. Yavuz, *A novel fractional-order model and analysis of cancer-immune system interaction in an avascular environment with an efficient control mechanism*, Journal of Computational and Applied Mathematics, 2026, 473, 1168887.

[32] H. Joshi, M. Yavuz and N. Ozdemir, *Analysis of novel fractional order plastic waste model and its effects on air pollution with treatment mechanism*, Journal of Applied Analysis and Computation, 2024, 14(6), 3078–3098.

[33] M. M. Kabir, et al., *Modified Kudryashov method for finding exact solitary wave solutions of higher-order nonlinear equations*, Mathematical Methods in the Applied Sciences, 2011, 34, 213–219.

[34] M. Kamrani, *Numerical solution of stochastic fractional differential equations*, Numer. Algorithms, 2015, 68, 81–93.

[35] M. M. A. Khater, A. R. Seadawy and D. Lu, *Dispersive optical soliton solutions for higher order nonlinear Sasa–Satsuma equation in mono mode fibers via new auxiliary equation method*, Superlattices and Microstructures, 2018, 113, 346–358.

[36] S. S. S. Kilic, *Multi and breather wave soliton solutions and the linear superposition principle for generalized Hietarinta equation*, International Journal of Modern Physics B, 2022, 36(2), 2250019.

[37] D. Kumar, A. R. Seadawy and A. K. Joardar, *Modified Kudryashov method via new exact solutions for some conformable fractional differential equations arising in mathematical biology*, Chinese Journal of Physics, 2018, 56, 75–85.

[38] C. Li and J. Llibre, *Uniqueness of limit cycles for Lienard differential equations of degree four*, J. Diff. Eqs., 2012, 252(4), 3142–3162.

[39] J. F. Li, H. Jahanshahi, S. Kacar, Y. M. Chu, J. F. Gómez-Aguilar, N. D. Alotaibi, et al., *On the variable-order fractional memristor oscillator: Data security applications and syn-*

chronization using a type-2 fuzzy disturbance observer-based robust control, Chaos Solitons Fractals, 2021, 145, 110681.

[40] X. Li and X. Yang, *Error estimates of finite element methods for stochastic fractional differential equations*, J. Comput. Math., 2017, 35, 346–362.

[41] F. Liu, V. Anh and I. Turner, *Numerical solution of the space fractional Fokker–Planck equation*, J. Comput. Appl. Math., 2004, 166, 209–219.

[42] J. Liu and L. Yan, *Solving a nonlinear fractional stochastic partial differential equation with fractional noise*, J. Theor. Probab., 2016, 29, 307–347.

[43] J. G. Liu, L. Zhou and Y. He, *Multiple soliton solutions for the new* $(2+1)$*-dimensional Korteweg–de Vries equation by multiple exp-function method*, Applied Mathematics Letters, 2018, 80, 71–78.

[44] J. Q. Mei and H. Q. Zhang, *New types of exact solutions for a breaking soliton equation*, Chaos Solitons Fractals, 2004, 20, 771–777.

[45] R. Metzler and J. Klafter, *The random walk's guide to anomalous diffusion, a fractional dynamics approach*, Phys. Rep., 2000, 339(1), 1–77.

[46] H. A. Mezban and H. A. Sultan, *The effect of the noise on the dynamics of soliton generation in microresonator*, AL-Muthanna Journal of Pure Science, 2024, 11(1).

[47] W. W. Mohammed, *Approximate solutions for stochastic time-fractional reaction diffusion equations with multiplicative noise*, Math. Methods Appl. Sci., 2021, 44(2), 2140–2157.

[48] W. W. Mohammed, et al., *The analytical solutions of the stochastic fractional Kuramoto–Sivashinsky equation by using the Riccati equation method*, Math. Probl. Eng., 2022, 1–8.

[49] W. W. Mohammed, H. Ahmad, H. Boulares, F. Khelifi and M. El-Morshedy, *Exact solutions of Hirota–Maccari system forced by multiplicative noise in the Itô's sense*, J. Low. Freq. Noise Vib. Act. Control, 2021, 14613484211028100.

[50] W. W. Mohammed, H. Ahmad, A. E. Hamza, E. S. ALy and M. El-Morshedy, *The exact solutions of the stochastic Ginzburg–Landau equation*, Results Phys., 2021, 23, 103988.

[51] W. W. Mohammed, S. Albosaily, N. Iqbal and M. El-Morshedy, *The effect of multiplicative noise on the exact solutions of the stochastic Burgers equation*, Waves Random Complex Media, (in press). DOI: 10.1080/17455030.2021.1905914.

[52] W. W. Mohammed, M. Alesemi, S. Albosaily, N. Iqbal and M. El-Morshedy, *The exact solutions of stochastic fractional-space Kuramoto–Sivashinsky equation by using the* G'/G*-expansion method*, Mathematics, 2021, 9, 2712.

[53] W. W. Mohammed, O. Bazighifan, M. M. Al-Sawalha, A. O. Almatroud and E. S. Aly, *The influence of noise on the exact solutions of the stochastic fractional-space chiral nonlinear Schrödinger equation*, Fractal Fract., 2021, 5, 262.

[54] W. W. Mohammed and N. Iqbal, *Impact of the same degenerate additive noise on a coupled system of fractional space diffusion equations*, Fractals, 2022, 30(1).

[55] W. W. Mohammed, N. Iqbal, A. Ali and M. El-Morshedy, *Exact solutions of the stochastic new coupled Konno–Oono equation*, Results Phys., 2021, 21, 103830.

[56] W. W. Mohammed, N. Iqbal and T. Botmart, *Additive noise effects on the stabilization of fractional-space diffusion equation solutions*, Mathematics, 2022, 10, 130.

[57] W. W. Mohammed and M. El-Morshedy, *The influence of multiplicative noise on the stochastic exact solutions of the Nizhnik–Novikov–Veselov system*, Math. Comput. Simulation, 2021, 190, 192–202.

[58] M. H. M. Moussa and A. A. Gaber, *Symmetry analysis and solitary wave solutions of nonlinear ion-acoustic waves equation*, International Journal of Analysis and Applications, 2020, 18, 448–460.

[59] P. A. Naik, A. Ahmad, Q. A. M. Farooq, M. Farman, A. Ghaffar, K. S. Nisar, A. Sambas and Z. Huang, *Dynamics of lumpy skin disease with treatment and viral factor monitoring through fractional operator*, Modeling Earth Systems and Environment, 2025, 11, 349.

[60] P. A. Naik, M. Ahmad and A. Zada, *Analyzing the soliton waves in the space-time fractional (2+1)-dimensional Calogero–Degasperis equation*, International Journal of Dynamics and Control, 2026, 14(1), 25.

[61] P. A. Naik, S. Naveen, V. Parthiban, S. Qureshi, M. Alquran and M. Senol, *Advancing Lotka-Volterra system simulation with variable fractional order Caputo derivative for enhanced dynamic analysis*, Journal of Applied Analysis and Computation, 2025, 15(2), 1002–1019.

[62] I. Podlubny, *Fractional Differential Equations*, Academic Press, New York, 1999.

[63] C. Prevòt and M. Röckner, *A Concise Course on Stochastic Partial Differential Equations*, Springer, 2007.

[64] M. Raberto, E. Scalas and F. Mainardi, *Waiting-times and returns in high-frequency financial data: An empirical study*, Physica A, 2002, 314, 749–755.

[65] M. M. Rasid, M. M. Miah, A. H. Ganie, H. M. Alshehri, M. S. Osman and W. X. Ma, *Further advanced investigation of the complex Hirota-dynamical model to extract soliton solutions*, Modern Physics Letters B, 2024, 38(10), 2450074.

[66] Y. Sabbar, *Enhanced analysis of general noncontinuous stochastic epidemic model with vaccination: A novel framework and practical application to COVID-19 in Saudi Arabia*, Communications in Nonlinear Science and Numerical Simulation, 2025, 149, 108911.

[67] Y. Sabbar, W. Adel and A. Elsonbaty, *Refining extinction criteria in a complex multi-stage epidemic system with non-Gaussian Lévy noise*, Mathematical Methods in the Applied Sciences, 2025, 48(6), 6734–6748.

[68] A. I. Saichev and G. M. Zaslavsky, *Fractional kinetic equations: Solutions and applications*, Chaos, 1997, 7(4), 753–764.

[69] S. Salahshour, A. Ahmadian, S. Abbasbandy, et al., *M-fractional derivative under interval uncertainty: Theory, properties and applications*, Chaos Solitons Fractals, 2018, 117, 84–93.

[70] M. M. Al-Sawalha, H. Yasmin, R. Shah, A. H. Ganie and K. Moaddy, *Unraveling the dynamics of singular stochastic solitons in stochastic fractional Kuramoto-Sivashinsky equation*, Fractal and Fractional, 2023, 7(10), 753.

[71] B. K. Singh, *Fractional reduced differential transform method for numerical computation of a system of linear and nonlinear fractional partial differential equations*, International Journal of Open Problems in Computer Science and Mathematics, 2016, 9(3), 20–38.

[72] Z. Taheri, S. Javadi and E. Babolian, *Numerical solution of stochastic fractional integro-differential equation by the spectral collocation method*, J. Comput. Appl. Math., 2017, 321, 336–347.

[73] H. Tajadodi, Z. A. Khan, A. R. Irshad, J. F. Gómez-Aguilar, A. Khan and H. Khan, *Exact solutions of conformable fractional differential equations*, Results Phys., 2021, 22, 103916.

[74] A. M. Wazwaz, *Integrable* $(2+1)$*-dimensional and* $(3+1)$*-dimensional breaking soliton equations*, Phys. Scr., 2010, 81, 035005.

[75] W. Wyss, *The fractional Black–Scholes equation*, Fract. Calc. Appl. Anal., 2000, 3, 51–61.

[76] H. Yasmin, A. S. Alshehry, A. H. Ganie, A. Shafee and R. Shah, *Noise effect on soliton phenomena in fractional stochastic Kraenkel-Manna-Merle system arising in ferromagnetic materials*, Scientific Reports, 2024, 14(1), 1810.

[77] H. Yépez-Martínez, J. F. Gómez-Aguilar and A. Atangana, *First integral method for non-linear differential equations with conformable derivative*, Math. Model. Nat. Phenom., 2018, 13.

[78] S. B. Yuste, L. Acedo and K. Lindenberg, *Reaction front in an* $A+B \to C$ *reaction subdiffusion process*, Phys. Rev. E, 2004, 69.

[79] S. B. Yuste and K. Lindenberg, *Subdiffusion-limited* $A+A$ *reactions*, Phys. Rev. Lett., 2001, 87(10–11).

[80] G. M. Zaslavsky, *Chaos, fractional kinetics and anomalous transport*, Phys. Rep., 2002, 371(6), 461–580.

[81] P. Yan-Ze, *New exact solutions for* $(2+1)$*-dimensional breaking soliton equation*, Commun. Theor. Phys., 2005, 43, 205–207.

[82] S. Zhang, *New exact non-traveling wave and coefficient function solutions of the* $(2+1)$*-dimensional breaking soliton equations*, Phys. Lett. A, 2007, 368, 470–475.

[83] G. Zou, *Galerkin finite element method for time-fractional stochastic diffusion equations*, Comput. Appl. Math., 2018, 37(4), 877–898.

Received September 2025; Accepted January 2026; Available online February 2026.